THEORY OF ELECTRON CYCLOTRON RESONANCE HEATING I: SHORT TIME AND ADIABATIC EFFECTS

by

F. Jaeger, A. J. Lichtenberg and M. A. Lieberman

Memorandum No. ERL-M305

3 September 1971

Electronics Research Laboratory

College of Engineering
University of California, Berkeley
94720

THEORY OF ELECTRON CYCLOTRON RESONANCE HEATING I: SHORT TIME AND ADIABATIC EFFECTS

F. JAEGER[†], A. J. LICHTENBERG and M. A. LIEBERMAN

Department of Electrical Engineering and Computer Sciences
and the Electronics Research Laboratory,
University of California, Berkeley, California 94720

ABSTRACT

The theory of single particle electron cyclotron resonance heating in a magnetic mirror is treated analytically and numerically, using the techniques of (a) integration of the Lorentz force equation and (b) transformation to a Hamiltonian approximation, to study both short time scale and adiabatic effects. The force equation is analytically integrated in the vicinity of the resonance plane to obtain the energy dependence of the effective time spent in resonance per bounce t_e. For electrons passing through the resonant zone at constant parallel velocity v_{zR}, $t_e \propto v_{zR}^{-1/2}$. For electrons which turn in or near the resonant zone, $t_e \propto v_{\perp R}^{-P}$, $P = 2/3$, where $v_{\perp R}$ is the transverse velocity at resonance. These results agree with the exact numerical integration of the force equation, for which $P \approx 0.5\text{-}0.7$.

Electron heating is limited by the existence of invariants at high energies, which present adiabatic barriers to the heating. The calculation of the barrier location is considered in a Hamiltonian theory of electron cyclotron heating, using the technique of resonance breakdown

---

[†]Present address: National Center for Atmospheric Research, Boulder, Colo., U.S.A.

of adiabatic invariance due to secondary island formation. It is found that resonance between the fifth harmonic of the energy oscillation and the half-bounce period τ_b (appearance of five islands) is sufficient to destroy the invariant. For a parabolic mirror $B(z) = B_0(1+z^2/L^2)$, the field necessary to destroy the invariant at a given energy is given by $eEL > 1.81\ (\tau_s/\tau_b)W_{\perp R}$, where e is the electronic charge, E the rf electric field, $W_{\perp R}$ the transverse electron energy at resonance, and τ_s is the period for the cyclotron phase to slip 2π with respect to the rf field. This result is in good numerical agreement with exact calculations.

I. INTRODUCTION

It has long been recognized that resonance between gyrofrequency and an rf wave can rapidly accelerate charged particles to high energy. However, ROBERTS and BUCHSBAUM (1964), treating the problem relativisticly, showed that even in a uniform field at exact resonance the relativistic change in mass detunes the frequency, thus generally leading to a limittation in the energy gain. Furthermore, confined particles are not in uniform fields, and thus would only be in resonance for part of the time during their motion. Just as off resonance particles have phase oscillations with respect to the accelerating field, and therefore energy oscillations, it might be expected that energy oscillations take place on a longer time scale if the particles oscillate in and out of resonance. SEIDL (1964) investigated this possibility, and showed that, for modest excursions about the resonant frequency and an energy gain per pass through resonance small compared to the total particle energy, invariants of the motion could exist. These limited the energy excursions, creating an energy oscillation on a time scale slow compared to the period at which the particle returned to the resonance region (bounce period for a magnetic mirror, which was the case treated by Seidl). TUMA and LICHTENBERG (1967) and LICHTENBERG et al (1969) investigated the phenomenon numerically, confirming Seidl's results within the validity of his theory, but also showing that for large excursions from resonance and large energy excursions per pass through resonance, the energy no longer appeared to oscillate, and the phase of the rf with respect to the particle at resonance appeared to be random, rather than ordered as predicted by Seidl's theory.

An entirely different approach to the problem was taken by BRAMBILLA (1968), KUCKES (1968A) and CANNOBIO (1968). They performed an integration through the resonant region from an initial magnetic field in which the phase difference was rapidly varying to a final field in which the phase was again rapidly varying. They showed that the energy change in this process could be considered to consist of three parts: a rapidly oscillating part dependent on the instantaneous phase, a part dependent on the initial phase, and a part independent of phase. The latter two parts were considered to be the non reversible or "nonadiabatic" portion of the energy gain. In calculating the energy gain over many traversals of resonance, Kuckes further assumed that the initial phase for each successive pass was random and concluded that the energy change dependent on initial phase would therefore not lead to an average energy change. He therefore calculated an average energy increase as the product of the number of times a particle transversed the resonant region times the non phase dependent energy gain per traversal. This general procedure was also used by GRAWE (1969) to calculate the energy gain of electrons in the Oak Ridge magnetic mirror device. However, while Kuckes assumed that the electron's parallel velocity was constant in successive traversals of the resonance region, Grawe considered that the transverse energy gain on successive traversals resulted in the particle turning around within or before the resonance region, with the penetration decreasing with energy. This effect was enhanced in Grawe's analysis by including the relativistic shift in cyclotron frequency, which further shifts the gyration frequency at the turning point away from resonance. Other calculations by KUCKES (1968B) indicate that the rf magnetic force

(ignored by Grawe) causes significant acceleration along the lines of force, which result in continued particle penetration of the resonant region. Numerical studies presented in Section 2 of this paper also indicate that the particles are not forced out of the resonance zone as predicted by Grawe. Although the heating predicted by Grawe was consistent with the experimental results (GRAWE, 1969), theoretical difficulties considered in Section 3 of this paper and in a companion paper (LIEBERMAN and LICHTENBERG, 1971B), in addition to the one discussed by Kuckes, indicate that his result may be somewhat fortuitous.

In all of the work discussed in the preceeding paragraph there are two basic difficulties; one is the lack of determination of the region of validity of stochastic acceleration (random phase assumption) and the other is the ignoring of geometrical effects in velocity space and the phase dependent energy diffusion. LICHTENBERG et al (1969) considered both of these questions. They showed numerically that a transition did occur between stochastic and adiabatic behavior. In the region predicted numerically to be stochastic, large energy gains were in fact observed in a pulsed electron cyclotron heating experiment (LICHTENBERG et al, 1969; TUMA et al, 1969). They also demonstrated that the energy dependence of the heating gave rise to a component of heating and an energy spread from the phase dependent acceleration of the same order as that arising from the phase independent acceleration. Their results were only of qualitative validity, in that the form of the distribution function was assumed rather than calculated from a solution to the Fokker-Planck equation. In Section 3 of LIEBERMAN and LICHTENBERG (1971 B), henceforth referred to as II, the Fokker-Planck equation is derived and the time dependence of the

distribution function and the average energy gain is obtained. The results obtained are in agreement with numerical calculations.

Stochastic heating is limited by the existence of invariants at high energies. These invariants present an adiabatic barrier to the heating of particles. The transition between adiabatic and non-adiabatic regions was investigated for cyclotron heating by LICHTENBERG and JAEGER (1970). The general mechanism for the resonance breakdown of adiabatic invariance has been investigated by CHIRIKOV (1960), ROSENBLUTH et al (1966), WALKER and FORD (1969) and by JAEGER and LICHTENBERG (1971). We apply the method to the cyclotron heating problem in Section 3. This is done by transforming to variables which are slowly varying compared to the explicit time dependence and then averaging over the time variable. This procedure, developed by BOGOLIUBOV and MITROPOLSKY (1961), eliminates the time dependence from the Hamiltonian, which is then a constant of the motion. Successive averaging over other rapidly varying variables introduces additional constants of the motion. The procedure is essentially the one used by SEIDL (1964). However, at each stage in the averaging, resonances between the fast oscillation and harmonics of the slow oscillation may modify or destroy the invariant. An isolated resonance may be removed by transformation to new variables, resulting in modified invariants, while strongly interacting resonances result in destruction of the invariants.

The transition between stochastic heating and oscillatory energy changes for cyclotron heating is closely allied to a wide class of problems in which particles are subject to periodic, impulsive forces

(ZASLAVSKII and CHIRIKOV, 1965; and LIEBERMAN and LICHTENBERG, 1971A). Following a rough criterion for stochasticity found by Zaslavskii and Chirikov, NEKRASOV (1970) obtained a criterion for the limit of stochastic heating. In II, we employ the more exact methods of Lieberman and Lichtenberg 1971A, to considerably sharpen this criterion. The approximations required to obtain an impulsive heating model are considered, and the adiabatic barrier to particle heating is derived. The results obtained are in substantial agreement both with the Hamiltonian approximation of this present paper and with exact numerical solutions. The averaging and expansion procedure in the Hamiltonian approximation results in mappings between resonances that are area preserving and thus different in character from the impulse approximation. However, despite this fundamental difference, the results are quite similar in most important respects.

We note that the treatment in this paper is for single particles, which generally holds for the plasma frequency less than the electron cyclotron frequency. This condition is often satisfied in ECRH experiments (LICHTENBERG et al, 1969, SPROTT, 1971). For experiments with high gas pressure, the plasma frequency generally builds up only to the level of the cyclotron frequency, beyond which the plasma may act to shield out the applied field, changing the character of the heating. The formalism which we develop is also applicable to ion heating, provided the proper fields are used. However, in this case, the self consistent properties of the plasma are usually important and we therefore have emphasized electron heating. Another interesting case of applicability is that in which the heating fields are self generated, for example, a single quasi-flute mode of fluctuation in a mirror machine (ROSENBLUTH, 1971). Here, as in the case of ion heating, the

self consistent plasma properties must be considered.

2. EQUATIONS OF MOTION

A. Exact Numerical Integration of the Equations of Motion

The most complete solution for the motion of charged particles in combined dc magnetic and rf electromagnetic fields is a numerical integration of the relativisticly correct equations of motion

$$\frac{d\underset{\sim}{r}}{dt} = \underset{\sim}{v}, \tag{1}$$

$$\frac{d\underset{\sim}{v}}{dt} = \frac{e}{m_0\gamma}\left[\underset{\sim}{E} + \underset{\sim}{v} \times \underset{\sim}{B} - \frac{\underset{\sim}{v}}{c^2}(\underset{\sim}{E}\cdot\underset{\sim}{v})\right] \tag{2}$$

where

$$\gamma = \left(1 - \frac{v^2}{c^2}\right)^{-1/2}.$$

For motion in a magnetic mirror, the dc magnetic field is approximated near the mirror axis $r < L'$ by

$$B_{0x} = -\frac{x}{r}\, b\, B_0' \frac{\pi r}{L'} \sin\frac{2\pi z}{L'}$$

$$B_{0y} = -\frac{y}{r}\, b\, B_0' \frac{\pi r}{L'} \sin\frac{2\pi z}{L'}$$

$$B_{0z} = B_0'\left[1 - \left[1 + \left(\frac{\pi r}{L'}\right)^2\right] b \cos\frac{2\pi z}{L'}\right], \tag{3}$$

where $r^2 = x^2 + y^2$, $b = (R_m - 1)/(R_m + 1)$, R_m is the mirror ratio, $B_0'(1 - b)$ is the magnetic field at the midplane, and $z = \pm L'/2$ are the locations of the magnetic mirrors.

For a given electromagnetic field, the six simultaneous differential equations (1) and (2) can be solved by standard numerical techniques on a computer. For simplicity a transverse electromagnetic wave propagating in the z direction is considered, of the form

$$\underset{\sim}{E} = E_0[\cos(\omega t - kz + \phi)\underset{\sim}{\hat{x}} \mp \sin(\omega t - kz + \phi)\underset{\sim}{\hat{y}}]$$

$$\underset{\sim}{B} = \frac{E_0}{c}[\sin(\omega t - kz + \phi)\underset{\sim}{\hat{x}} \pm \cos(\omega t - kz + \phi)\underset{\sim}{\hat{y}}], \tag{4}$$

where by proper choice of signs and amplitudes, circularly polarized, linearly polarized, traveling and standing waves can be considered. These fields correspond to practical heating configurations and are appropriate to compare with various analytic heating models.

Exact computations are very convenient for phenonema that occur on the time scale of the cyclotron period, rather time consuming for practical orbits in mirror devices where the phenomena occur on the time scale of the bounce period ($10\tau_c < \tau_b < 10^3\tau_c$), and not very useful for longer time scales. This allows for a detailed investigation of resonance phenomena, an adequate method of treating energy oscillations for particles oscillating in an out of a resonant region, and only very sketchy treatment of stochastic heating in which the longitudinal oscillation causes phase randomization with respect to the resonant rf wave.

We have previously used numerical plots of the energy-phase relation at successive resonance crossings to illustrate the different character of adiabatic and stochastic behavior (LICHTENBERG et al, 1969). In Section 3 of this paper and in Sections 2 and 3 of II, the exact computations are used, as far as possible, to confirm the results of the

approximate calculations determining the transition between adiabatic and stochastic behavior and the properties of stochastic heating. The computations are made to compare with phenomena on all time scales, with the results successivly limited as the time scale becomes larger.

In Fig. 1 we plot graphs of the energy gain versus time for two electrons of different energies confined in a magnetic mirror and accelerated by a strong electromagnetic field that resonates with the cyclotron frequency within the mirror region. In Fig. 1a, the injection energy is low, 30 eV both perpendicular and parallel to the magnetic field, and the electric field is sufficiently strong to raise the perpendicular energy to approximately a kilovolt after the first pass through resonance. From these calculations one observes that the parallel energy remains fairly constant within the resonance region. On successive transits, the energy perpendicular to the magnetic field may either increase or decrease, depending sensitively on the phase at resonance. The particle is also seen to turn within the resonance region provided the particle's energy remains large. This is understandable, in that the parallel energy at resonance does not change greatly, and thus the mirror force turns the particle near resonance whenever the perpendicular energy at resonance has become large compared to the parallel energy. We shall put these ideas on a more quantitative basis in the next subsection. The type of orbit illustrated in Fig. 1a is one in which stochastic heating can take place, on a longer time scale, and we shall treat this case in detail in II.

In Fig. 1b, the injection energy is higher, the applied electric field smaller, and we observe that the particle's energy remains approximately constant over times long compared to the bounce period. This be-

havior is evidence of the existence of a new adiabatic invariant of the motion, replacing the magnetic moment, which constrains the particle energy. We deal with the theory of this motion in Section 3, and investigate the transition between the types of motion in Figs. 1a and 1b, from two different points of view, in Section 3 and in Section 2 of II.

B. Analytic Expressions

We now obtain expressions for the half-bounce time (time between collisions) and the time spent in the resonance zone, that will be useful for later calculations. The half-bounce time in the absence of the rf field is given by

$$\tau_b = 2 \int_0^{\ell} \frac{dz}{\left[\frac{2}{m}\left(W - \mu B(z)\right)\right]^{1/2}}$$

where W is the total energy and μ the magnetic moment (both assumed constant) of the particle, and ℓ is the value of z at the turning point. Substituting for μ at $B(\ell) = B_{max}$, then $\frac{1}{2}mv_{\perp\ell}^2 = W$, and W can be removed from the integral in the form

$$\tau_b = \frac{2}{W^{1/2}} \int_0^{\ell} \frac{dz}{\left[\frac{2}{m}\left(1 - \frac{B(z)}{B_{max}}\right)\right]^{1/2}} \tag{5}$$

which shows that τ_b scales as $W^{-1/2}$ or $v_{\perp\ell}^{-1}$. For a parabolic magnetic field of the form

$$B = B_0(1 + z^2/L^2),$$

(5) can be integrated to yield

$$\tau_b = \pi L(1 + \ell^2/L^2)/v_{\perp\ell}. \tag{6}$$

The effective time a particle spends in the resonance zone can be obtained by solving the equation of motion of the electron in the neighborhood of resonance. We choose a local coordinate with z = 0 at resonance, and which is assumed to be locally linear: $B_z(z) = B(1 + \alpha z)$; $B_r = -\frac{1}{2} B\alpha r$. We consider a circularly polarized wave with the electric field rotating in the same direction as the particle under study. In a system of reference that is rotating with the particle; i.e., introducting the complex notation $h_\perp = \frac{1}{\sqrt{2}} (h_x - ih_y)$, the Lorentz force law is:

$$\frac{d}{dt} v_\perp + i\omega_c v_\perp = -\frac{e}{m} E_\perp + iv_z(\omega_\perp + \Omega_\perp) \tag{7}$$

$$\frac{d}{dt} v_z = iv_\perp (\omega_\perp^* + \Omega_\perp^*) - iv_\perp^*(\omega_\perp + \Omega_\perp), \tag{8}$$

where

$$\omega_c = \frac{eB_z}{m} = \omega(1+\alpha z),$$

$$\omega_\perp = \frac{e}{m} B_\perp = -\omega \frac{\alpha r_\perp}{2},$$

$$r_\perp = \frac{r}{\sqrt{2}} e^{-i\psi},$$

$$\Omega_\perp = \frac{e}{m} \tilde{B}_\perp = -i \frac{kc}{\omega} \frac{eE_\perp}{mc},$$

and where $E_\perp$ and $\tilde{B}_\perp$ represent the electric and magnetic fields of the wave.

In many experimental situations, the following inequalities hold:

$$\left|\frac{kv_z}{\omega}\right|, \left|\frac{kv_\perp}{\omega}\right|, \left|\frac{\alpha v_z}{\omega}\right|, \left|\frac{\alpha v_\perp}{\omega}\right| << 1. \tag{9}$$

The first two hold if the electron velocities are slow compared to the phase velocity of the wave, which is generally true for electron cyclotron heating to non-relativistic velocities. Under these conditions, the longitudinal and transverse forces due to the wave magnetic field can be neglected in (7) and (8). These forces are also neglected in the Hamiltonian approximation in Section 3, but included in the exact numerical computation of Section 2A. KUCKES (1968B) has examined the effect of these terms on the particle motion for relativistic energies. The second two inequalities above are valid provided that the electron larmor radius and the longitudinal distance traveled during a cyclotron period are both small compared to the scale length of the dc field. Under these conditions, the forces due to the magnetic field inhomogeneity (mirror forces) can be described in the adiabatic limit and to a first approximation can be neglected in (7). One then has:

$$\frac{d}{dt} v_\perp + i\omega(1+\alpha z)v_\perp \simeq -\frac{e}{m} E_\perp, \tag{10}$$

$$\frac{d}{dt} v_z \simeq a_0, \tag{11}$$

where $a_0 = \mu_0 \alpha B/m$ and $\mu_0 = \frac{1}{2} mv_\perp^2(0)/B$. Solving (11) subject to the initial condition that $z(0) = \Delta z$ and $v_z(0) = 0$ yields

$$v_z(t) = \Delta z - a_0 t$$

$$z(t) = \Delta z - \frac{1}{2} a_0 t^2. \tag{12}$$

Inserting (12) into (10), and introducing the change of variables $v_\perp(t) = V_\perp(t)e^{-i\omega t}$ and $E_\perp(t) = \varepsilon_\perp e^{-i\omega t}$, we obtain the differential equation

$$\frac{dV_\perp}{dt} + i\Omega(t)V_\perp = -\frac{e}{m}\varepsilon_\perp, \tag{13}$$

where $\Omega = \omega\alpha(\Delta z - \frac{1}{2} a_0 t^2)$. The solution to (13) with the initial perpendicular velocity specified at $t = -T$, and the final velocity determined at $t = T$ is

$$V_\perp(T) = V_P + V_\perp(-T), \tag{14}$$

where

$$V_P = -\frac{e}{m}\varepsilon_\perp e^{-i\theta(t)} \int_{-T}^{T} e^{i\theta(t')}dt' \tag{15}$$

and

$$\theta = \omega\alpha(t\Delta z - \frac{1}{6} a_0 t^3). \tag{16}$$

The above specification insures that the initial and final energy are measured at the same axial position $z = \Delta z - \frac{1}{2} a_0 T^2$. Putting $V_P = |V_P|e^{i\phi_P}$ and $V_\perp(-T) = |V_\perp(-T)|e^{i\phi_0}$, we see that (16) describes an energy gain in the form

$$|V_\perp(T)|^2 = |V_\perp(-T)|^2 + |V_P|^2 + 2|V_P||V_\perp(-T)|\cos(\phi_0-\phi_P), \quad (17)$$

showing both a phase-independent and a phase-dependent heating.

As we will see, the energy gain is acquired in a narrow zone around the resonant position z = 0. Provided T is chosen sufficiently large, then $|V_P|$ is insensitive to the exact choice of T, and we can write

$$|V_P| = \frac{e}{m} |E_\perp| t_e, \quad (18)$$

where t_e is the effective time the particle spends in resonance, given by

$$t_e = \left| \int_{-\infty}^{\infty} \cos(\omega\alpha\Delta z t - \frac{1}{6} \omega\alpha a_0 t^3) dt \right|. \quad (19)$$

This can be expressed in terms of the Airy function as

$$t_e = 2\omega^{-1}\Gamma \, |Ai(x)|, \quad (20)$$

where

$$x = - \Gamma\alpha\Delta z,$$

$$\Gamma = \left(\frac{2\omega}{\alpha v_{\perp R}}\right)^{2/3}, \quad (21)$$

$v_{\perp R}$ is the transverse velocity at resonance, and in view of (9), $\Gamma >> 1$.

We now discuss the behavior of the effective time t_e, which is a factor in determining the rate of particle heating in the mirror field.

A graph of Ai(x), given in Fig. 2 is useful for this purpose. We distinguish three different forms of particle-field interaction, depending on the location of the turning point with respect to the point of resonance. For $\Delta z > 0$, the particle passes through exact resonance at $z = 0$, turns at $z = \Delta z$, and then again passes through resonance. It is convenient to introduce the parallel velocity at exact resonance, v_{zR}. From (12), $v_{zR}^2 = 2a_0 \Delta z$, so that $x = -\Gamma v_{zR}^2 / v_{\perp R}^2$ in (20). There are two cases to consider, depending on the magnitude of x. Before the microwave heating field is applied, we expect that most of the particles trapped in the mirror which also pass through the position of exact resonance have $v_{zR}^2 > \Gamma^{-1} v_{\perp R}^2$; ie, $|x| > 1$. This will be true for the usual Maxwellian or mirror loss cone distributions. For $x \leq -1$, we can expand the Airy function in an asymptotic series to obtain

$$t_e = 2\pi^{-1/2} \left(\frac{2}{\alpha v_{zR} \omega} \right)^{1/2} \left| \sin\left(\frac{2}{3} x^{3/2} + \frac{\pi}{4} \right) \right| . \qquad (22)$$

The oscillation in t_e as x varies (see also Fig. 2) is the beating which results from the two successive passes through resonance for the parabolic orbit given by (12). If we had considered a single pass through resonance, this oscillation would not be present. The result in (22), taking the peaks of the oscillation, agrees with that of KUCKES (1968A), who calculated the energy gain of an electron in a linear magnetic field, assuming a constant parallel velocity v_{zR}, for a single pass through resonance. In this case, as (22) shows, we expect a particle with low velocity along the field lines to gain more energy than a higher velocity particle, since it spends more time in resonance.

If the particle continues to gain perpendicular energy, v_{zR} remaining constant, it turns closer and closer to the position of exact resonance. The detailed motion depends on the existence and location of an absolute velocity barrier, possible particle losses, parallel velocity diffusion of particles, etc. If these processes do not limit the perpendicular energy gain, we eventually obtain the condition $v_{\perp R}^2 \gtrsim \Gamma\, v_{zR}^2$ for a large group of particles; ie, $|x| \lesssim 1$. (There is also a small group of particles for which $v_{\perp R}^2 \gtrsim \Gamma\, v_{zR}^2$ initially.) In this case, Fig. 2 shows that $Ai(x) \approx A(0) = .355$, so that

$$t_e \approx .71\omega^{-1}\Gamma. \tag{23}$$

We now find that t_e is independent of v_{zR}. Substituting for Γ from (21), we find that t_e is inversely proportional to $v_{\perp R}^{2/3}$; ie, the higher the particle's transverse energy, the less efficiently it is heated.

If $v_{\perp R}$ continues to increase, then the assumption that v_{zR} is a constant is not fulfilled and the $\mu\nabla B$ force within the resonance region may result in the particle turning before the point of exact resonance ($\Delta z < 0$). There is also another small group of particles for which this is true when the microwave heating field is first applied. From the form of Ai(x) for positive x, we see that the heating falls off rapidly as $|\Delta z|$ increases for this case. Expanding the Airy function for large positive argument, we find

$$t_e \approx .565\omega^{-1}\Gamma\, x^{-1/4}\exp(-\tfrac{2}{3}x^{2/3}), \tag{24}$$

where $x = \Gamma\alpha|\Delta z| \gtrsim 1$; the heating falls off exponentially as $|\Delta z|$ increases.

We estimate the effective width w of the heating zone for the limit (22) of deep penetration as $w \approx v_{zR} t_e$. For turning near the point of resonance, from (23) and (24), we estimate $w \approx \Delta z$ when $x \approx 1$; ie, $w \approx \Gamma^{-1}\alpha^{-1}$. In both cases, making use of the inequalities (19), we find that

$$\alpha w << 1; \tag{25}$$

namely, the width w of the zone is much smaller than the scale length α^{-1} of the dc field variation. We also note that in all cases,

$$\omega t_e >> 1; \tag{26}$$

ie, the particle makes many cyclotron gyrations in the resonance region. In view of (25), we can choose the integration time T in (15) such that

$$t_e << T << \tau_b, \tag{27}$$

where τ_b is the time between collisions with the resonant zone. The inequality (27) insures that the replacement $T \to \infty$ in (19) is valid.

The scaling of τ_b and t_e can be tested numerically from the exact equations of motion. We consider typical energy trajectories of particles in the stochastic region as shown in Fig. 1a. The time τ_b between successive crossings of the midplane and the time t_e' spent in the resonant zone, defined by a phase shift of π between the rf and cyclotron phases, are determined numerically. We note that t_e' is closely related to the effective time spent in resonance t_e. Measuring τ_b and t_e' over a wide range of energy, the results are given in Fig. 3. These results are

found to agree well with proportionality (6) for τ_b, and to the proportionality (23) for t_e applicable to particles turning within the resonance zone. We also justify the assumption that $v_{zR} \cong$ constant for successive resonance crossings from the numerical data. In Fig. 4, $v_{\perp R}/c$ (triangles) and v_{zR}/c (crosses), the values at resonance crossing, are plotted for two particles with different initial conditions. The parallel velocity is seen to remain relatively constant, while the perpendicular velocity may increase to a large value. For particle 1 there was a slow increase in parallel energy at resonance, while for particle 2 (encircled points), the parallel velocity decreased slightly and failed to reach exact resonance on the last three passes. In both cases, the perpendicular velocity changes included a random phase governing the acceleration, but particle 1, by chance, gained energy nearly continuously.

3. HAMILTONIAN APPROXIMATION

A. Basic Equations

In the absence of the electromagnetic fields, the particle motion can be approximately transformed to action-angle variables such that the motion in each of the three degrees of freedom (cyclotron, longitudinal, drift) can be considered separately (LACINA, 1963). SEIDL (1964) extended the treatment to include the rf field as a perturbation and demonstrated that for sufficiently small rf fields, new invariants of the motion exist which prevent particle heating. In this section, Seidl's treatment is extended to larger fields. For this situation, the invariants may not exist, in which case the particles may gain energy. The important result is the calculation of a transition energy between

adiabatic and nonadiabatic behavior, which predicts an energy barrier, as a function of applied field, beyond which particles cease to be heated.

We calculate the transition from adiabatic to nonadiabatic behavior using the method of resonance modification of invariants of JAEGER and LICHTENBERG (1971) and following Seidl's treatment of cyclotron heating. We use orthogonal coordinates as shown schematically in Fig. 5. All lengths are normalized to ℓ, the half-length between mirror points. The magnetic field B is assumed parabolic, $B/B_0 = 1 + a\eta^2$, where $a = \ell^2/L^2$ and $\eta = z/\ell$. Following Seidl, we designate action variables for the Larmor, azimuthal, and longitudinal motions, P_1, P_2 and P_3 respectively. The corresponding angle variables are w_1, w_2 and w_3. P_3 is equivalent to the longitudinal action integral

$$P_3 = \frac{1}{2\pi} \oint p_\eta \, d\eta \tag{28}$$

and w_3 is the phase of the longitudinal oscillation so that $\eta = \eta_m \sin w_3$, where η_m is the maximum longitudinal penetration, which can be shown to be $\eta_m^2 = (2/a)^{1/2} \, P_3/P_1^{1/2}$. Similarly, w_2 is the phase angle for the azimuthal drift of the guiding center and P_2 is proportional to the flux through the drift orbit. The angle w_1 is related to the Larmor angle Q_1 by the relation

$$Q_1 = w_1 - \frac{1}{4} \frac{P_3}{P_1} \sin 2w_3 \tag{29}$$

such that the longitudinal variation of the Larmor motion has been subtracted out to make $\nu_1 = \dot{w}_1$ the average value of the Larmor frequency

over a longitudinal bounce, rather than the instantaneous value. In the midplane where $w_3 = 0$, P_1 is proportional to the magnetic moment $\mu = W_\perp/B$. Hence P_1 is proportional to the perpendicular energy $W_{\perp o}$ in the midplane. In terms of P_1, P_2, P_3, w_1, w_2, and w_3, an expansion in powers of P_2 yields

$$H_0 = \omega_o P_1 \left[\gamma_0(P_2) + \gamma_1(P_2) \frac{P_3}{P_1^{1/2}} + \gamma_2(P_2) \left(\frac{P_3}{P_1^{1/2}} \right)^2 + \cdots \right] \qquad (30)$$

where ω_o is the Larmor frequency at the midplane,

$$\gamma_0(P_2) = 1 - aP_2 - \frac{1}{2} a^2 P_2^2$$

$$\gamma_1(P_2) = (2a)^{1/2} (1 + aP_2 - 3a^2 P_2^2 + \ldots)$$

$$\gamma_2(P_2) = 10\, a^2 P_2 (1 - 4aP_2 + \frac{9}{2} a^2 P_2^2 + \cdots),$$

and P_1 and P_2 are related to the particle energy in the midplane by

$$W_{\perp o} = m\omega_o^2 L^2 \gamma_0(P_2) P_1$$

$$W_{zo} \tilde{=} m\omega_o^2 L^2 \left[\gamma_1(P_2) P_3 P_1^{1/2} + \gamma_2(P_2) P_3^2 \right]. \qquad (31)$$

We note that (30) is independent of w_1, w_2, w_3, and time t, so that P_1, P_2, P_3, and H_0 are constants of the motion.

If we add to the system a radio frequency electric field propagating parallel to the magnetic field; this rf field can be treated as a per-

turbation on the original Hamiltonian H_0 so that

$$H = H_0(P_1,P_2,P_3) - \varepsilon\ \omega_o\ H_1\ (w_1,w_3,P_1,P_3,\omega t) \tag{32}$$

where

$$H_1 = P_1^{1/2} \cos(w_1 - \frac{1}{4}\frac{P_3}{P_1} \sin 2w_3)\ \cos(kL\eta_m \sin 2w_3)\sin \omega t \tag{33}$$

and

$$\varepsilon = \sqrt{2}\,\frac{E}{\omega B_o L} \tag{34}$$

and ω, E and k are the frequency, amplitude, and wave number of the electric field.

The dependence of the Hamiltonian on the time can be removed by transforming to a new phase variable $w_1' = w_1 - \omega t + Nw_3$, where N is the number of 2π phase slippages per complete period of longitudinal oscillation ($2\tau_b$). The angle w_1' is slowly varying with respect to ωt, so we can then average over ωt. The procedure employs the method of averaging, as developed by BOGOLIUBOV and MITROPOLSKY (1961). Although the limits of validity of the method have not been established, recent work of JAEGER and LICHTENBERG (1971) indicates that the method works provided the period $2\pi/\omega$ is at least a factor of five shorter than any other periodicity in the system. A canonical transformation to the new phase variable, using the generating function

$$F_2 = (w_1 - \omega t + Nw_3)P_1' + w_2P_2' + w_3P_3', \tag{35}$$

and performing the average, yields

$$\langle H \rangle_{\omega t} = \omega_o \left[(\gamma_0 - \omega/\omega_o)P_1 + \gamma_1 P_1^{1/2}(P_3' + NP_1) + \gamma_2(P_3' + NP_1)^2 + \frac{\varepsilon\omega_o P_1^{1/2}}{2} \sin(w_1' - \alpha \sin 2w_3)\cos(\beta \sin 2w_3)\right], \quad (36)$$

where $\alpha = \frac{1}{4} P_3/P_1$ and $\beta = kLn_m$. The primes have been omitted from all variables that are unchanged. Hamilton's equations can then be integrated numerically in time to obtain the particle trajectory, with the time scale for integration being on the order of a fraction of the bounce period, rather than a fraction of the cyclotron period. The procedure used by SEIDL (1964) to reduce the motion to quadratures is to assume that w_3 is rapidly varying with respect to w_1' and perform a second averaging. Resonances between harmonics of the slower oscillation and the fundamental of the bounce oscillation can locally distort the phase space, either modifying the existing invariants of the motion or destroying them altogether. We shall consider these topics in detail shortly.

An alternative to averaging over w_3 is to choose a fixed w_3 and examine the phase plane at successive crossings of w_3 = Const. This technique is useful for numerically determining the existence of invariants. Here, we reverse the procedure, assuming adiabatic invariance, and demonstrate that we can plot $P_1 - w_1'$ in a surface of section, giving answers very similar to the values obtained after averaging. We start from (36), substitute appropriate constants for $\langle \bar{H} \rangle_{\omega t}$ and chose w_3 at resonance ($\sin 2w_3 = (-1)^n$ for the unperturbed system). With

these substitutions, (36) becomes

$$P_1 + (P_1)^{1/2}(P_3 - NP_1) - \frac{\omega}{\omega_o} P_1 + \epsilon \frac{P_1^{1/2}}{2} \cos(kL\eta_m(-1)^n) \times \sin\left(w_1' - \frac{1}{4} \frac{(P_3 - NP_1)}{P_1}(-1)^n\right) = \text{Const.} \tag{37}$$

Provided P_3 is a constant of the motion, (37) will trace out a unique trajectory in the $P_1 - w_1'$ phase plane, representing a mapping of the curve of constant Hamiltonian into itself. This mapping can also be constructed directly from Hamilton's equations without requiring P_3 to be a constant. In this case, no simple $P_1 - w_1'$ phase curves may exist. However, the Hamiltonian nature of (36) insures that the mapping is area-preserving.

B. Results for Average over Bounce Oscillation

We consider the case of exact average resonance ($w_1' = w_1 - \omega t$) as treated by Seidl. Expanding the perturbation H_1 in a Fourier series, keeping only the slowly varying term,

$$H_1 = \frac{-P_1^{1/2}}{4i} \sum_{n=-\infty}^{\infty} \left\{ \left(\sum_{m=-\infty}^{\infty} \mathcal{J}_{2m}(\beta)\, \mathcal{J}_{n-2m}(\alpha) \right) \left(-e^{-iw_1'} + (-1)^n e^{iw_1'} + e^{-i(w_1' + 2\omega t)} - (-1)^n e^{i(w_1' + 2\omega t)} \right) \right\} e^{i2nw_3}, \tag{38}$$

where $\mathcal{J}$ is a Bessel function of order shown.

Averaging over w_3 and ωt, the total averaged Hamiltonian is

$$\bar{H} = \omega_o[\gamma_0 - \omega/\omega_o)P_1 + \gamma_1 \; P_1^{1/2} \; P_3 + \gamma_2 P_3^2] + \varepsilon \; \omega_o \frac{P_1^{1/2}}{2} f(P_1,P_3)\sin w_1', \tag{39}$$

where

$$f = \sum_{m=-\infty}^{\infty} \mathcal{J}_{2m}(\alpha) \; \mathcal{J}_{2m}(\beta).$$

Since $\bar{H}$ is independent of w_3, the lowest order adiabatic invariant is

$$P_3 \simeq \text{constant}. \tag{40}$$

This is the main conclusion of Seidl's work. We note that the range of validity of the averaging is considerably more restricted here than in Section 3A, as the average is not only over the fastest variable with frequency ω but also over the slower longitudinal variable with bounce frequency w_3. We check the accuracy of the average over w_3, by comparing the slow P_1, w_1' oscillation from (39) (Fig. 6a), with numerical integration from (36) before the average over w_3 but after the average over ωt (Fig. 6b). The numbers in Fig. 6b represent successive crossings of a plane of section in w_3,

$$\sin 2w_3 = 1.0. \tag{41}$$

There are approximately six longitudinal bounces for each oscillation in the perpendicular energy P_1, the particle crossing a resonance twice during each longitudinal period. The slight scatter in the points plotted is due to inaccuracies in satisfying (41) exactly. The relatively smooth curves traced out in the $P_1 - w_1'$ phase plane indicate the existence of an adiabatic invariant which in this case we know is P_3 to lowest order. The values of P_3, averaged over a longitudinal bounce are plotted in Fig. 7 for one of the phase loops of Fig. 6b, and we see that P_3 is approximately constant and equal to its initial value of 4×10^{-4}. As a further check on the theory, we have integrated the exact equations of motion (1) and (2) numerically for parameters corresponding to Fig. 6b. The good agreement between the phase space plot of the exact numerical calculation in Fig. 6c with the Hamiltonian result in Fig. 6b indicates that the Hamiltonian approximation is valid. The agreement between Figs. 6a and 6b, which shows that the average over the bounce is valid, holds for the very low value of ϵ (field perturbation) chosen, for which the energy gain per pass through resonance is very small compared to the total energy of the particle. Since the particle energy is proportional to P_1, we see that the energy oscillates and continuous heating does not take place. In the next sections, we examine the case for somewhat larger value of ϵ in which the bounce average is not valid, and determine a criterion for the validity of the averaging.

C. Second Order Resonances and Invariant Destruction

In Figs. 8a, b and c, we plot trajectories similar to Figs. 6a, b and c, except that the value of ϵ has been increased sufficiently for a

chain of islands to appear surrounding the closed phase orbits, indicating a significant bounce-energy resonance. We include the exact numerical calculation in Fig. 8c, for the island chain only, to demonstrate that islands can be observed in the absence of any approximations, although the islands may not be stable over long times. A plot of P_3 averaged over the longitudinal oscillation for the island trajectory is shown in Fig. 9. P_3 oscillates with the period of the island oscillation as is shown by the numbering of the points. Points 11-16 lie on the inside of the islands in Fig. 6b and hence enclose a small area inside their phase loop. We see from Fig. 9 that these same points have relatively low values of P_3. On the other hand, points 21-26 lie on the outside of the islands enclosing a larger area inside their phase orbit, and we see from Fig. 9 that these points have relatively high values of P_3.

To explain the behavior exhibited in these figures, it is necessary to treat the higher order resonance in the system which in this case is the bounce-energy resonance. We transform to the action-angle variables of the P_1 oscillation; i.e., solve the Hamilton-Jacobi equation

$$\bar{H}(\partial S/\partial w_1', w_1', P_2, P_3) = \bar{H}(J_1, P_2, P_3), \tag{42}$$

where $S(w_1', J_1)$ is the partial generating function to transform to action-angles J_1, θ_1. As in Section 3A, we expand the average Hamiltonian, $\bar{H}$, about the elliptic singular point $\overline{P_1}$, $\overline{w_1'}$. The average part of the Hamiltonian in action-angle variables is then of the form

$$\bar{H} = \omega_o\{[\gamma_0(P_2) - \omega/\omega_o]\,\overline{P_1} + \gamma_1(P_2)\,\overline{P_1}^{1/2}P_3 + \gamma_2(P_2)P_3^2\}$$
$$+ F(P_3) - \Omega^0(P_3)J_1[1 - \lambda^2(J_1, P_3)M(P_3)] \tag{43}$$

where Ω^0 is the lowest order energy oscillation frequency, $\lambda = (2J_1R)^{3/2}/(2\Omega^0 J_1) \propto \epsilon^{1/2}$, and we have written J_2 and J_3 as P_2 and P_3 respectively, since these variables are unchanged by the transformation. F, R, Ω^0 and M are functions of P_3 resulting from the expansion which are derived in Appendix 1. The varying part of the Hamiltonian can be Fourier analyzed as

$$\tilde{H}_1 = -\frac{\bar{P}_1^{1/2}}{4} \sum_{\substack{\ell,n \\ n\neq 0}} S_n(\bar{P}_1,P_3)[(-1)^\ell + (-1)^n] \; \mathcal{J}_\ell[(2J_1/R)^{1/2}]\exp(i\ell\theta_1 + 2inw_3) \tag{44}$$

where

$$S_n(\bar{P}_1,P_3) = \sum_{m=-\infty}^{\infty} \mathcal{J}_{2m}(\bar{\beta}) \; \mathcal{J}_{n-2m}(\bar{\alpha})$$

and $\bar{\alpha}$ and $\bar{\beta}$ are defined as in (38) except with $\bar{P}_1$ replacing P_1. The total Hamiltonian is

$$H = \bar{H}(J_1,P_2,P_3) - \epsilon\omega_0 \tilde{H}_1(J_1,P_2,P_3,\theta_1,w_3) \tag{45}$$

where $\bar{H}$ and $\tilde{H}$ are given by (43) and (44) respectively.

If we now define the unperturbed frequencies:

$$\bar{\nu}_3(J_1,P_2,P_3) = \partial\bar{H}/\partial P_3 = \text{longitudinal bounce frequency} \tag{46}$$

$$\bar{\Omega}(J_1,P_2,P_3) = \partial\bar{H}/\partial J_1 = \text{energy oscillation frequency,} \tag{47}$$

we see from the exponential argument in (44) that there can be resonances in (45) of the form $\bar{\nu}_3/\bar{\Omega} = \frac{1}{2}$ r/s. These resonances will introduce secularities in the time rate of change of the simple adiabatic invariant P_3.

The resonances only occur for certain values of J_1 and P_3 which in general may vary due to the secularities. As we see in Fig. 8b, islands form around elliptic singularities in the J_1,θ_1 plane. Hence we can transform to coordinates $(\hat{\theta}_1,\hat{w}_2,\hat{w}_3,\hat{J}_1,\hat{P}_2,\hat{P}_3)$ in which $\hat{\theta}_1$ is the difference phase $2sw_3 + r\theta_1$, which is slowly varying near the elliptic singularity. The required generating function is

$$F_2 = (2sw_3 + r\theta_1)\hat{J}_1 + w_2\hat{P}_2 + w_3\hat{P}_3, \tag{48}$$

which defines the transformation to the hat variables in the rotating frame,

$$\begin{aligned}
\hat{\theta}_1 &= \partial F_2/\partial \hat{J}_1 = 2sw_3 + r\theta_1 \qquad & J_1 &= \partial F_2/\partial\theta_1 = r\hat{J}_1 \\
\hat{w}_2 &= \partial F_2/\partial \hat{P}_2 = w_2 & P_2 &= \partial F_2/\partial w_2 = \hat{P}_2 \\
\hat{w}_3 &= \partial F_2/\partial \hat{P}_3 = w_3 & P_3 &= \partial F_2/\partial w_3 = \hat{P}_3 + 2s\hat{J}_1.
\end{aligned} \tag{49}$$

Writing the perturbation (44) in terms of the hat variables and averaging over $\hat{w}_3$, we get

$$\tilde{\tilde{H}} = -\frac{\bar{\bar{P}}_1^{1/2}}{4} \sum_{\substack{\ell,n \\ n\neq 0 \\ nr-\ell s=0}} S_n(\bar{\bar{P}}_1,\hat{P}_3 + 2s\hat{J}_1)[(-1)^{\ell} + (-1)^{n}]\ \mathcal{J}_{\ell}[(2r\hat{J}_1/R)^{1/2}]\exp[i\ell\hat{\theta}_1/r]. \tag{50}$$

The double bar average corresponds to keeping just the most slowly varying terms which, for the $\bar{\nu}_3/\bar{\Omega} = \frac{1}{2}$ r/s resonance, are the ℓ = jr and n = js terms where j runs over all positive integers.

The total average Hamiltonian taking into account the bounce-energy

resonance can now be written as

$$\bar{\bar{H}} = \omega_o[(\gamma_0(\hat{P}_2) - \omega/\omega_o)\bar{P}_1 + \gamma_1(\hat{P}_2)\bar{P}_1^{1/2}(\hat{P}_3 + 2s\hat{J}_1) + \gamma_2(\hat{P}_2)(\hat{P}_3 + 2s\hat{J}_1)^2]$$

$$+ F(\hat{P}_3,\hat{J}_1) - \Omega^0(\hat{P}_3,\hat{J}_1)r\hat{J}_1[1-\lambda^2(\hat{P}_3,\hat{J}_1)M(\hat{P}_3,\hat{J}_1)] \qquad (51)$$

$$+ \varepsilon\omega_o \frac{\bar{P}_1^{1/2}}{2} \sum_{j=1}^{\infty} S_{js}(\hat{P}_3,\hat{J}_1)[(-1)^{jr} + (-1)^{js}]\ \mathcal{J}_{jr}[(2r\hat{J}_1/R)^{1/2}]\cos j\hat{\theta}_1,$$

where all quantities are derived in the appendix. Since $\bar{\bar{H}}$ is independent of $\hat{w}_3$, the correct adiabatic invariant for the island case is

$$\hat{P}_3 = P_3 - 2sJ_1/r \simeq \text{constant}, \qquad (52)$$

which reduces to the invariant P_3 for a very high order resonance, $r >> s$. Since $\bar{\bar{H}}$ in (51) is independent of time, we can use $\bar{\bar{H}}$ = constant together with $\hat{P}_3$ = constant to plot $\hat{J}_1$ versus $\hat{\theta}_1$ for various values of $\bar{\bar{H}}$. Rather than do this directly, we see from (52) that if J_1 oscillates, then P_3, the adiabatic invariant without resonances, must also oscillate. This explains the sychronized oscillation between P_3 and J_1 observed in comparing Figs. 8b and 9. We plot the oscillation in P_3, $\hat{\theta}_1$ for the five island resonance as solid lines in Fig. 10. The inner bold curve corresponds to the initial conditions of the five island trajectory in Fig. 8b. On the right hand axis we give the ratio ν_3/Ω. The oscillation centers about an average bounce-energy resonance number of $\nu_3/\Omega = 2.5$, as does the five island trajectory in the numerical integration. At the extremes of the oscillation, the ratio ν_3/Ω never moves very far from 2.5, going to 2.54 at the top of the phase loop and 2.46 at the bottom, thus justi-

fying the fundamental assumption for keeping only the most slowly varying terms, that the system should remain close to a particular bounce-energy resonance.

In the numerical integrations of Fig. 8b, we also find relatively smooth phase loops near the elliptic singular point and ergodic trajectories beyond the islands. By plotting P_3, $\hat{\theta}_1$ phase diagrams for these other types of behavior, we can distinguish the physical mechanism that differentiates among them. The most slowly varying term for the islands ($\nu_3/\Omega = 2.5$) had ℓ=5, n=1 in the sum (44), plus higher harmonics. Taking r=7 and s=1 leads to the much smaller oscillation about ν_3/Ω = 3.5 shown as the family of dot-dashed curves at the top of Fig. 10. Also, r=3, s=1 contributes the drifting oscillations shown as dashed lines. (The integral resonances ν_3/Ω = r/2s = 1,2,3, ... lead only to extremely small oscillations in the adiabatic invariant P_3, and are not considered). The bold dot-dashed and dashed drifting curves in Fig. 10 correspond to the 9/2 and 3/2 resonances, respectively, for the island oscillation of Fig. 8b. In the remaining discussion, we focus the discussion solely on the bold curves, corresponding to the initial conditions of Fig. 8b. Close to the 2.5 resonance, the drifting curves of Fig. 10 average nearly to zero over an island oscillation. To see this, we recall that the nonresonant terms average exactly to zero when the system is right at the 2.5 resonance due to the orthogonality of the exponentials making up the Fourier series (44). If the system is not exactly at resonance, the nonresonant terms do contribute, but in the approximation of a symmetric oscillation about resonance, the contributions above and below resonance cancel. The assumption of symmetry

around the resonance is valid in the linear region close to the island singularity, so that the total nonresonant contribution averages nearly to zero over the island oscillation. Thus the double bar average (51) with r = 5 and s = 1 is a reasonable approximation for the island trajectory in Fig. 8b.

For the ergodic trajectory in Fig. 8b, shown as unconnected numbers, the nonresonant terms do not average to zero since the system is not close enough to the 2.5 resonance. The random trajectory, being a combination of the bold curves in Fig. 11, lies between the 2.5 and 3.5 resonances, and is not close enough to either resonance to justify keeping only one term in the sum. Furthermore, P_3 cannot remain constant in this case because of the large variations introduced by the r/2s = 3/2 term. This term will also be rapidly varying with respect to the natural bounce-energy frequency of the system which is approximately 2.72; the net result is a random mixing of the three rapidly varying terms r/2s = 3/2, 5/2, and 7/2, leading to the ergodic behavior observed.

If we plot P_3, $\hat{\theta}_1$ phase diagrams for one of the relatively well behaved phase loops near the elliptic singularity of Fig. 8b, we find that although there is no single dominant slowly varying term, none of the terms introduces significant variation in P_3, as seen in Fig. 12. This result is to be expected, as the strength of the near resonant harmonic terms is proportional to Bessel functions depending on $J_1^{1/2}$. The amplitudes of the harmonics decrease rapidly with decreasing action J_1.

If we compare the amplitude of the oscillation in P_3 as shown by Fig. 9 to the amplitude of the 2.5 island oscillation given by the bold

curve in Fig. 10, we see that the observed variation in P_3 is a factor of 2 to 3 times larger than the value predicted by removing the higher order resonance. An underestimation of the variation of P_3 is to be expected, since we have overestimated the nonlinearity by expanding the average Hamiltonian to only fourth order in ΔP and Δw. The next term would be of opposite sign, thus reducing the nonlinearity and making the amplitude of the predicted island oscillations larger. We note, however, that even if the phase loops in Fig. 10 were 2 to 3 times larger in amplitude, the variation in P_3 would still be only 1/5 to 1/3 of that necessary for marginal overlap between the 2.5 and 3.5 resonances. The actual overlap of neighboring island oscillations is not necessary for breakdown to occur. Rather, it is only necessary that the islands be close enough that a phase orbit between the two resonances is affected significantly by both terms, as is the case in Fig. 11.

D. Limits of Stochastic Acceleration

In the previous subsection, we have explored the condition for the breakdown of the invariants of the motion. This condition is, in fact, complementary to the limit of stochastic acceleration, for it is the existence of invariants that create curves of constant Hamiltonian which bound the stochastic orbits. We now proceed to obtain simple approximate criteria for the limits of stochastic behavior.

The results of the previous subsection indicate that breakup occurs when the width of the second order resonances is approximately equal to 1/3 the resonance separation. Calculations performed on other systems give similar results (JAEGER and LICHTENBERG, 1971). This criterion can be written

$$\frac{r}{\Omega}\frac{d\Omega}{dJ}\,2\hat{J}_{max} = \frac{1}{3}, \tag{53}$$

where Ω is the frequency of the first order resonance at which the r^{th} harmonic resonates with twice the bounce frequency, and $\hat{J}_{max}$ is the island amplitude (half the island width). We can simplify $\bar{\bar{H}}$ in (51) to obtain to lowest order in ε and in the nonlinearity

$$\bar{\bar{H}} = \Omega_0\hat{J} + \frac{r}{2}\frac{\partial\Omega}{\partial\bar{J}}\,\hat{J}^2 + \varepsilon\,\delta(\bar{J})\cos\,\hat{\theta} = \text{const.}, \tag{54}$$

where

$$\delta(\bar{J}) = \frac{r}{2}\,\omega_o\bar{P}_1^{1/2}S_1\;\mathcal{J}_r[(2\bar{J}/R)^{1/2}]. \tag{55}$$

It follows that

$$\hat{J}_{max} = 2\left(\frac{\varepsilon\,\delta(\bar{J})}{r\,\frac{\partial\Omega}{\partial\bar{J}}}\right)^{1/2}, \tag{56}$$

such that (53) becomes

$$\Omega^{-1}\left[\varepsilon\; r\delta(\bar{J})\partial\Omega/\partial\bar{J}\right]^{1/2} = 1/12\ . \tag{57}$$

Substituting for all values from Appendix 1, keeping only lowest order terms in ε, setting $S_1 = 1$, and $\mathcal{J}_r[2\bar{J}/R] = 1/r!$ (an over estimation), (57) simplifies to

$$3\sqrt{2}r(r!)^{-1/2} = 1. \tag{58}$$

On the left, we have 1.9 for r = 5 and .95 for r = 6. This result is in good agreement with the observed relatively unstable island formation for

r = 5. Similar calculations on other multidimensional systems also indicate that the invariants cease to exist for second order resonance numbers of approximately this value.

Although the equations in Section 3B describe the case of exact average resonance (N = 0), closely analogous results hold for the more general case in which there are 2N additional 2π phase slippages within each bounce. Here we briefly consider this more general case to demonstrate the similarity in the criterion for invariance breakdown and the stochastic acceleration limit; and to derive some simple formulae from which the adiabatic orbits and the stochasticity limit can be calculated.

From (36), with $\varepsilon = 0$, we obtain the unperturbed resonance condition $\partial \langle H \rangle_{\omega t} / \partial P_1 = 0$; namely,

$$\omega_o - \omega + \omega_o (a/2P_1)^{1/2} P_3 + N\omega_o (2aP_1)^{1/2} = 0, \tag{59}$$

from which we can obtain P_3 as a function of P_1 at resonance. The unperturbed bounce frequency ν_3 and the linearized energy oscillation frequency Ω_0 can also be found from (36). Differentiating (36) with respect to P_3 with $\varepsilon = 0$, we obtain

$$\nu_3 = \omega_0 (2aP_1)^{1/2}. \tag{60}$$

To obtain Ω_0 we first pick out the resonant term in (36), obtained as in (39):

$$\langle H_1 \rangle_{w_3} = \omega_o P_1^{1/2} f_n(\bar{P}_1, P_3) \sin w_1', \tag{61}$$

where

$$f_n = (-1)^n \sum_m \mathcal{J}_{n-2m}(\alpha) \quad \mathcal{J}_{2m}(\beta).$$

The dominant term in f_n is generally m = 0, which gives

$$f_n \simeq (-1)^n \, \mathcal{J}_n\left(\frac{1}{4}\frac{P_3}{\bar{P}_1}\right) \tag{62}$$

In the linear approximation, we can calculate the frequency of adiabatic orbits from $\Omega_0 = (FG)^{1/2}$ (LICHTENBERG, 1969), where $F = \partial^2 H/\partial w_1^2$ and $G = \partial^2 H/\partial P_1^2$ are the lowest order terms of the linearized Hamiltonian. We find

$$\Omega_0 = \frac{\omega_o}{2}\left[\left|\frac{\varepsilon}{2} f \left(\frac{P_3}{\bar{P}_1} - 3N\right) (2a)^{1/2}\right|\right]^{1/2}. \tag{63}$$

Similarly, the elliptic phase space trajectory is given by

$$\Delta P_1 = (F/G)^{1/2}(\phi^2 - \phi_1^2)^{1/2} \tag{64}$$

where, in lowest order

$$\left(\frac{F}{G}\right)^{1/2} = \left[\left|\frac{2\,\varepsilon\,\bar{P}_1 f_n}{-\frac{P_3}{\bar{P}_1} + 6N}\right|\right]^{1/2} \tag{65}$$

and ϕ_1 is the phase at which $P_1 = \bar{P}_1$ ($\Delta P_1 = 0$).

We now use (63) to obtain an approximate overlap criterion, with the results equivalent to those for the case of exact average resonance (N = 0). Numerical calculations for the case of $2\pi N$ slippage, although not as ex-

tensive as those carried out for N = 0, indicate that the adiabatic orbits are destroyed at a low order resonance between the bounce motion and the energy oscillation, of the form

$$\nu_3/\Omega_0 = r/2, \tag{66}$$

where r is an integer between 4 and 6. Because of symmetry considerations the even harmonic interactions are considerably weaker than the odd harmonics (LICHTENBERG and JAEGER, 1970) and we consider that r = 5 at the breakdown of adiabaticity.

We first compare this result for the value of the rf field necessary to obtain stochasticity with the numerical calculation of Fig. 8b. Substituting (60) and (63) into (66), with N = 0, and setting $f \simeq \frac{1}{2}$, we obtain

$$\epsilon = (8/r)^2 \, \bar{P}_1^2/P_3, \tag{67}$$

which, for the numerical values of the five island case of Fig. 8b, gives an $\epsilon \simeq 6.5 \times 10^{-5}$, which is in reasonable agreement with the $\epsilon = 4.7 \times 10^{-5}$ used in the five island calculation. If a somewhat smaller value of ϵ were used in the calculation, the five islands would appear closer to the elliptic singular point, corresponding more closely to the linear frequency used in the calculation of Ω_0 and thus giving better agreement. However, in this case, the Bessel function approximation leading to (58) would be a greater over estimation, and we would find that island overlap would not occur.

We can get a feeling for the magnitudes involved in the stochasticity criterion by substituting into (67) the physical parameters. The normalized action integrals are related to the physical parameters by (31) and

the additional relations $P_1 = \frac{1}{2}(r_{Lo}/L)^2$ and $P_2 = \frac{1}{2}(r_{go}/L)^2$, where r_{Lo} and r_{go} are the Larmor and guiding center radii measured at the midplane. A set of nonrelativistic parameters corresponding to Fig. 6 are λ = 30 cm, L = 6 cm, $v_{\perp o}/c = 1.8 \times 10^{-2}$, $v_{zo}/c = 3.7 \times 10^{-3}$, r_{go} = 2 cm, r_{Lo} = 8.5×10^{-2} cm, B_0 = .36 KG, and E = 4.5 V/cm. This is a weak electric field case which has also been scaled to low velocities. The breakup of the invariant curves, corresponding to Fig. 8, is for a field 5 times as large.

Returning to the more general case of $2\pi N$ phase slippages per bounce, we can obtain a condition analogous to (67) for the stochastic boundary. Combining the unperturbed resonance condition (59) with the assumption that $\eta_{res} = \eta_m$, then $\omega/\omega_o - 1 = 2N(2aP_1)^{1/2}$, and we find that $P_3 = 2NP_1$. Substituting this result into (63), (66) yields for the stochasticity condition

$$\varepsilon = 2(8/r)^2 P_1^2/P_3 \tag{68}$$

We note that (68) differs from (67) by a factor of two, because exact resonance is a special case that must be treated separately. However, since P_3 is considerably larger for $N \neq 0$ than for $N = 0$, (68) gives values of ε smaller at the stochastic barrier.

To obtain a physical feeling for the barrier conditions, and to facilitate calculations, we reintroduce the physical parameters from (31) and (34), to obtain

$$eEL > \frac{1}{\sqrt{2}}\left(\frac{8}{5}\right)^2 \frac{\tau_s}{\tau_b} W_{\perp R} \tag{69}$$

where $\tau_s = 2N\tau_b$ is the period for the gyration phase to slip through 2π radians with respect to the field in a half-bounce time τ_b. τ_s is related to the gyration period by a small numerical factor, which for the parabolic well is

$$\tau_s = \tau_{co}(L^2/\ell^2), \tag{70}$$

where τ_{co} is the cyclotron period at the bottom of the well and the resonant points are at $z = \pm \ell$. Therefore, except for a factor of order unity, the energy gain over the scale length of the system L must be greater than the particle energy by the ratio of the cyclotron period to the bounce period for the particle to be stochasticly heated. Although slightly less physical, a more practical form of (69) is given by solving for the energy in terms of the field. Substituting for τ_b from (6), we obtain

$$W_{\perp R} < 1.15(\hat{t}/\tau_s)^{2/3}\ eEL, \tag{71}$$

where $\hat{t}$ is a field dependent time given by

$$\hat{t} = \left[\frac{m}{eE} L\left(1 + \frac{\ell^2}{L^2}\right)\right]^{1/2}. \tag{72}$$

To illustrate these results with a practical example, we take the parameters of an electron cyclotron heating experiment previously reported (LICHTENBERG et al, 1969), for which $\tau_{co} = 10^{-10}$ sec, L = 15 cm, $\ell^2/L^2 = .25$ and $E = 10^3$ volts/cm (200 kw pulse transmitted into a 10 cm diameter chamber). Then $\tau_s = 4\tau_{co}$ from (70), $\hat{t} = 8.5\ \tau_s$ from (72), and from (71), we obtain the criterion for stochasticity that $W_{\perp R} < 70$ keV. This is well above the actual heating of ~ 10 keV measured experimentally.

However, for weaker fields or longer heating pulses (a 0.25 μsec pulse was used in the experiment) the heating limit can easily be reached.

We shall show in Section 3 of II that the experimental heating can be predicted very accurately from a stochastic theory. In Section 2 of II, the criterion for stochasticity (71) derived from the Hamiltonian theory is compared with a similar criterion obtained from an impulsive treatment of the rf field, and both criteria are compared with the results of exact numerical calculations. Anticipating this comparison, we find good agreement (within 30%) among the Hamiltonian, impulse and exact numerical calculations.

4. CONCLUSION

In conclusion, we have shown that the effective time a particle spends in resonance per bounce t_e for particles turning in the resonant zone is, from (23), $t_e \propto v_{\perp R}^{-2/3}$, where $v_{\perp R}$ is the transverse velocity at resonance. Numerically we have found that if the energy gain per pass through resonance is comparable to the initial particle energy, then the particle will turn in the resonance zone after the first or the first few bounces. Any theory of stochastic heating will therefore have to incorporate the $t_e \propto v_{\perp R}^{-2/3}$ law, and we do so in II, Section 3.

Using Hamiltonian theory we have shown that sufficient invariants may exist at high energy to create an energy barrier for a given field, beyond which stochastic heating cannot be maintained. The mechanism by which the invariants are destroyed is a resonance between the fifth harmonic of the slow energy oscillation and the half-bounce period. By examining the energy oscillation in the adiabatic approximation, the fifth harmonic resonance can easily be found, for a parabolic magnetic

well, in terms of the system parameters. For exact average resonance, we have shown that the result agrees well with exact numerical calculations. For the more general case of phase slippage, a relation between a given field strength and the limiting energy for which stochastic heating can be maintained is given in (71) and (72). In II, Section 2, these results will be shown to agree well with an impulse approximation and with an exact numerical integration of the equations of motion.

Acknowledgments -- We wish to acknowledge the help of C. Luk in making some of the numerical computations. This work was supported by the National Science Foundation under Grant GK-2978 and the Air Force Office of Scientific Research under Grant AFOSR-69-1754.

REFERENCES

BOGOLIUBOV, N. N. and MITROPOLSKY, Y. A. (1961) Asymptotic Methods in the Theory of Nonlinear Oscillations, Gordon and Breach, New York.

BRAMBILLA, M. (1968) Plasma Phys. 10, 359.

CANNOBIO, E. (1968) Plasma Phys. 10, 441.

CHIRIKOV, B. V. (1960) J. Nucl. Energy, Pt. C 1, 253.

GRAWE, H. (1969) Plasma Phys. 11, 151.

JAEGER, F. and LICHTENBERG, A. J. (1971) Ann. Phys. (N.Y.) ___, .

KUCKES, A. F. (1968A) Plasma Phys. 10, 367.

KUCKES, A. F. (1968B) Physics Lett. 26A, 599.

LACINA, J. (1963) Czech. J. Phys. B13, 401

LICHTENBERG, A. J. (1969) Phase Space Dynamics of Particles, John Wiley and Sons (Cha. 2).

LICHTENBERG, A. J. and JAEGER, F. (1970) Phys. Fluids 13, 392.

LICHTENBERG, A. J., SCHWARTZ, M. J. and TUMA, D. T. (1969) Plasma Phys. 11, 101.

LIEBERMAN, M. A. and LICHTENBERG, A. J. (1971A) Phys. Rev. ___, .

LIEBERMAN, M. A. and LICHTENBERG, A. J. (1971B) Plasma Phys. ___, .

NEKRASOV, A. K. (1970) Nuclear Fusion 10, 387.

ROSENBLUTH, M. N. (1971) private communication.

ROSENBLUTH, M. N., SAGDEEV, R. Z., TAYLOR, J. B. and ZASLAVSKY, G. M. (1966) Nucl. Fusion 6, 297.

SEIDL, M. (1964) Plasma Phys. (J. Nucl. Energy. Pt. C) 6, 597.

SPROTT, J. C. (1971) Phys. Fluids 14, 1795.

TUMA, D. T. and LICHTENBERG, A. J. (1967) Plasma Phys. 9, 87.

TUMA, D. T., LICHTENBERG, A. J. and TRIVELPIECE, A. W. (1969) Plasma Phys. 11. 117

WALKER, G. H. and Ford, J. (1969) Phys. Rev. 188, 416.

ZASLAVSKII, G. M. and CHIRIKOV, B. V., Soviet Physics Doklady 9, 989.

APPENDIX 1.

In this appendix, we expand the average Hamiltonian (39) about its elliptic singularity and use second order perturbation theory to transform to action-angle variables. Repeating (39),

$$\bar{H} = \omega_o\left[(\gamma_0 - \omega/\omega_o)P_1 + \gamma_1 P_1^{1/2} P_3 + \gamma_2 P_3^2\right] + \frac{1}{2}\varepsilon\omega_o P_1^{1/2} f(P_1,P_3)\sin w_1', \tag{A1}$$

we write Hamilton's equations

$$\dot{P}_1 = -\frac{\partial\bar{H}}{\partial w_1'} = -\frac{1}{2}\varepsilon\omega_o \bar{P}_1^{1/2} f(P_1,P_3)\cos w_1' \tag{A2}$$

$$\dot{w}_1' = \frac{\partial\bar{H}}{\partial P_1} = \omega_o\left[(\gamma_0 - \omega/\omega_o) + \frac{1}{2}\frac{\gamma_1 P_3}{P_1^{1/2}}\right] + \frac{1}{2}\varepsilon\omega_o\left(P_1^{1/2}\frac{\partial f}{\partial P_1} + \frac{1}{2}\frac{f}{P_1^{1/2}}\right)\sin w_1'. \tag{A3}$$

For the elliptic singularity $\bar{P}_1$, $\bar{w}_1'$, using (A2) and (A3), we obtain

$$\bar{w}_1' = \frac{\pi}{2} \tag{A4}$$

$$\left.\frac{\partial f}{\partial P_1}\right|_{\bar{P}_1} = \frac{-2}{\varepsilon\,\bar{P}_1^{1/2}}\left[(\gamma_0 - \omega/\omega_o) + \frac{\gamma_1 P_3}{2\,\bar{P}_1^{1/2}}\right] - \frac{f(\bar{P}_1,P_3)}{2\bar{P}_1} \tag{A5}$$

where (A5) must be solved numerically for $\bar{P}_1$. We expand the functions $f(P_1,P_3)$, $\bar{P}_1^{1/2}$, and $\sin w_1'$ about $\bar{P}_1$, $\bar{w}_1'$. Defining

$$\Delta P = P_1 - \bar{P}_1$$

$$\Delta w = w_1' - \bar{w}_1' \tag{A6}$$

we obtain

$$\bar{H} = \omega_o \left[(\gamma_0 - \omega/\omega_o)\bar{P}_1 + \gamma_1 \bar{P}_1^{1/2} P_3 + \gamma_2 P_3^2\right] + F(P_3)$$

$$- G(P_3)\frac{(\Delta P)^2}{2} - F(P_3)\frac{(\Delta w)^2}{2} + A(P_3)\frac{(\Delta P)^3}{3} + B(P_3)\frac{\Delta P(\Delta w)^2}{3} + I(P_3)\frac{(\Delta P)^4}{4}$$

$$+ D(P_3)\frac{(\Delta P)^2(\Delta w)^2}{4} + E(P_3)\frac{(\Delta w)^4}{4} \tag{A7}$$

where

$$F = \frac{1}{2}\omega_o \bar{P}_1^{1/2} f(\bar{P}_1,P_3)$$

$$G = \frac{\omega_o \varepsilon P_1^{1/2}}{2}\left(\frac{3\gamma_1 P_3/\varepsilon + 3f(\bar{P}_1,P_3)/2}{2\bar{P}_1^2} + \frac{2(\gamma_0 - \omega/\omega_o)}{\varepsilon \bar{P}_1^{3/2}} - \frac{\partial^2 f}{\partial P_1^2}\bigg|_{\bar{P}_1}\right)$$

$$A = \frac{\omega_o \varepsilon}{4\bar{P}_1^{1/2}}\left(\frac{3\gamma_1 P_3/\varepsilon + 3f(\bar{P}_1,P_3)/2}{2\bar{P}_1^2} + \bar{P}_1 \frac{\partial^3 f}{\partial P_1^3}\bigg|_{\bar{P}_1} + \frac{3}{2}\frac{\partial^2 f}{\partial P_1^2}\bigg|_{\bar{P}_1}\right.$$

$$\left. + \frac{3}{2}\frac{(\gamma_0 - \omega/\omega_o)}{\varepsilon \bar{P}_1^{3/2}}\right)$$

$$B = \frac{\omega_o \varepsilon \bar{P}_1^{1/2}}{2}\left(\frac{3(\gamma_0 - \omega/\omega_o)}{\varepsilon \bar{P}_1} + \frac{3\gamma_1 P_3}{2\varepsilon \bar{P}_1}\right)$$

$$I = \frac{-3\omega_o \varepsilon}{16\bar{P}_1^{3/2}}\left(\frac{3\gamma_1 P_3/\varepsilon + 3f(\bar{P}_1,P_3)/2}{2\bar{P}_1^2} + \frac{4(\gamma_0 - \omega/\omega_o)}{3\varepsilon \bar{P}_1^{3/2}} + \frac{2}{3}\frac{\partial^2 f}{\partial P_1^2}\bigg|_{\bar{P}_1}\right.$$

$$\left. - \frac{8}{9}\bar{P}_1 \frac{\partial^3 f}{\partial P_1^3}\bigg|_{\bar{P}_1} - \frac{4}{9}\bar{P}_1^2 \frac{\partial^4 f}{\partial P_1^4}\bigg|_{\bar{P}_1}\right)$$

$$D = \frac{\omega_o \varepsilon \bar{P}_1^{1/2}}{2}\left(\frac{2\gamma_1 P_3/\varepsilon + 3f(\bar{P}_1,P_3)/2}{2\bar{P}_1^2} + \frac{2(\gamma_0 - \omega/\omega_o)}{\varepsilon \bar{P}_1^{3/2}} - \frac{\partial^2 f}{\partial P_1^2}\bigg|_{\bar{P}_1}\right)$$

$$E = \frac{\omega_o \varepsilon \bar{P}_1^{1/2}}{2}\frac{f(\bar{P}_1,P_3)}{6}\,.$$

Since the first two terms on the left of (A7) do not depend on the variables P_1, w_1', they can be combined with H in determining the ΔP - Δw motion with P_2 and P_3 constant. The Hamilton-Jacobi equation for Hamiltonian (A7) becomes

$$-G(P_3)\frac{(\Delta P)^2}{2} - F(P_3)\frac{(\Delta w)^2}{2} + A(P_3)\frac{(\Delta P)^3}{3} + B(P_3)\frac{\Delta P(\Delta w)^2}{3} + I(P_3)\frac{(\Delta P)^4}{4}$$

$$+ D(P_3)\frac{(\Delta P)^2(\Delta w)^2}{4} + E(P_3)\frac{(\Delta w)^4}{4} = K(J_1,P_2,P_3)\cdot \qquad \text{(A8)}$$

We can now transform to action-angle variables J_1^0, θ_1^0 for the linear problem using the polar coordinate transformation

$$\Delta P = (2J_1^0 R)^{1/2} \cos \theta_1^0$$

$$\Delta w = (2J_1^0/R)^{1/2} \sin \theta_1^0,$$

for which (A8) becomes

$$\bar{H}_0(J_1^0) + \delta \bar{H}_1(J_1^0,\theta_1^0) + \delta^2 \bar{H}_2(J_1^0,\theta_1^0) = K(J_1,P_2,P_3), \tag{A9}$$

where

$$\bar{H}_0(J_1^0 = - \Omega^0 J_1^0$$

$$\bar{H}_1(J_1^0,\theta_1^0) = \lambda \left\{ \Omega^0 J_1^0 \frac{2}{3}(A\cos^3\theta_1^0 + \frac{B}{R^2} \cos \theta_1^0 \sin^2\theta_1^0) \right\}$$

$$\bar{H}_2(J_1^0,\theta_1^0) = \lambda^2 \left\{ \Omega^0 J_1^0 \frac{G}{2}(I\cos^4\theta_1^0 + \frac{D}{R^2} \cos^2\theta_1^0 \sin^2\theta_1^0 + \frac{E}{R^4} \sin^4\theta_1^0) \right\}$$

$$R = (F/G)^{1/2}, \ \Omega^0 = (FG)^{1/2}, \ \lambda = (2J_1 R)^{3/2}/2\Omega^0 J_1$$

and δ is an artificial constant measure of smallness. Using standard perturbation theory, we solve for the first order generating function

$$S_1 = \frac{2}{9} J_1 \lambda \sin \theta_1 \left[A(\cos^2\theta_1^0 + 2) + \frac{B}{R^2} (\sin^2\theta_1^0) \right], \tag{A10}$$

and the second order change in the energy,

$$K_2 = \Omega^0 J_1 \lambda^2 M(P_3), \tag{A11}$$

where

$$M(P_3) = \frac{3}{16} GI + \frac{1}{16}\frac{GD}{R^2} + \frac{3}{16}\frac{GE}{R^4} + \frac{5}{24} A^2 + \frac{1}{12}\frac{AB}{R^2} + \frac{1}{24}\frac{B^2}{R^4} .$$

The average Hamiltonian $\overline{H}$ in action-angle variables J_1,θ_1, valid to λ^2, is

$$\overline{H}(J_1,P_2,P_3) = \omega_o \left[(\gamma_0 - \omega/\omega_o)\overline{P}_1 + \gamma_1 \overline{P}_1^{1/2} P_3 + \gamma_2 P_3^2\right] + F(P_3)$$

$$- \Omega^0 J_1 (1-\lambda^2 M), \tag{A12}$$

and the frequency of the energy oscillation, $\dot{\theta}_1$, is

$$\dot{\theta}_1 = \frac{\partial \overline{H}}{\partial J_1} = - \Omega^0(P_3) \left[1-2\lambda^2(J_1,P_3)M(P_3)\right] . \tag{A13}$$

The nonlinearity in the energy oscillation prevents a secular increase in the action. The second order term in $S(J_1,\theta_1^0)$ is

$$S_2 = J_1\lambda^2 \left\{ \frac{G}{8} \sin\theta_1^0 \cos\theta_1^0 \left[I(\cos^2\theta_1^0 + \frac{3}{2}) + \frac{D}{R^2}(-\cos^2\theta_1^0 + \frac{1}{2})\right.\right.$$

$$\left. + \frac{E}{R^4}(-\sin^2\theta_1^0 - \frac{3}{2})\right] + \frac{2}{3} \sin\theta_1^0 \cos\theta_1^0 \left[A^2(\frac{1}{6}\cos^4\theta_1^0\right.$$

$$\left. + \frac{5}{24}\cos^2\theta_1^0 + \frac{5}{15}) + \frac{AB}{R^2}(\frac{1}{3}\cos^2\theta_1^0 \sin^2\theta_1^0\right.$$

$$- \frac{1}{4} \cos^2\theta_1^0 + \frac{1}{8}) + \frac{B^2}{R^4} (\frac{1}{6} \sin^4\theta_1^0 - \frac{1}{24} \sin^2\theta_1^0 - \frac{1}{16}) \Big] \Big\}, \tag{A14}$$

from which we obtain the transformation from variables ΔP, Δw to action-angle variables J_1, θ_1 correct to second order in δ. As a check of this transformation, it can be substituted into (A8) to verify that this equation is satisfied.

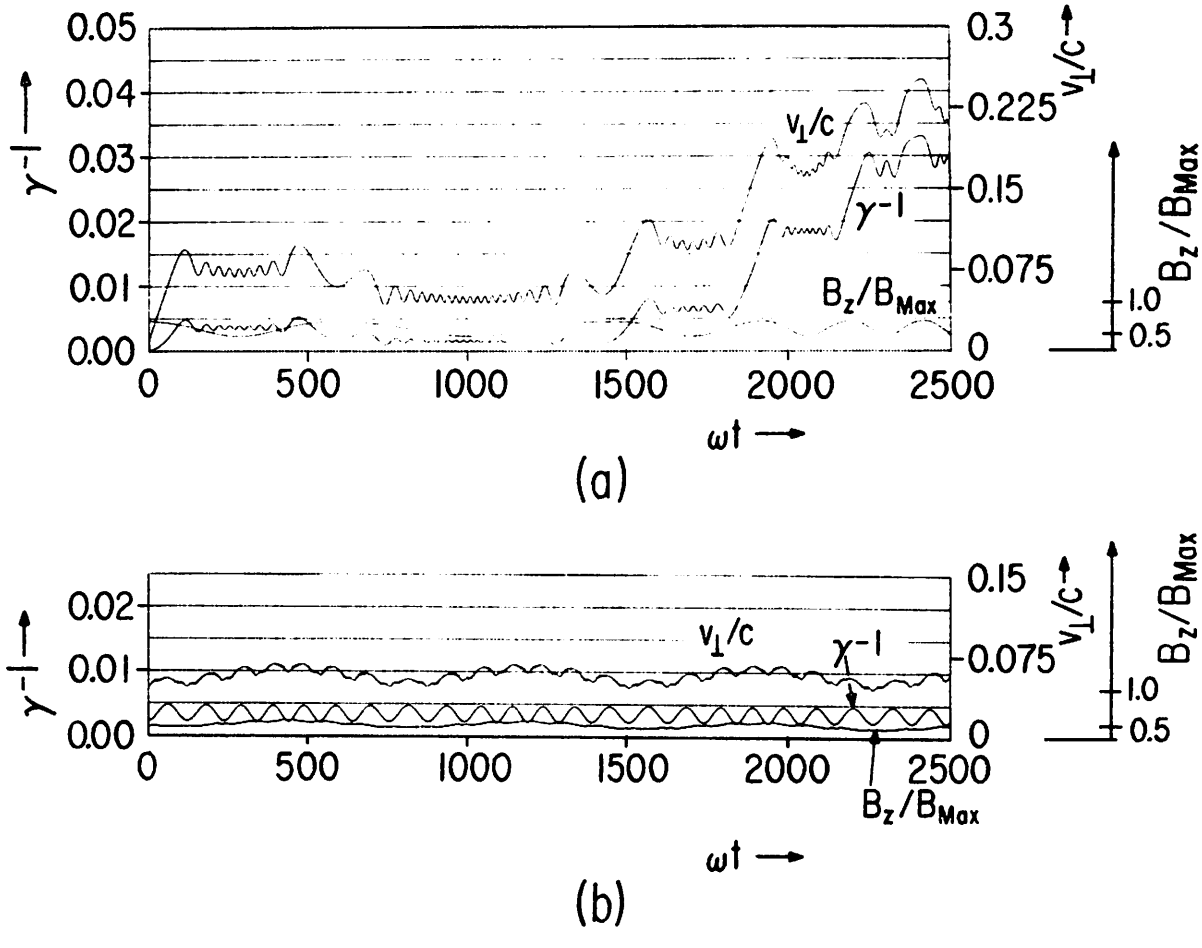

Fig. 1. Energy gain vs. time. γ-1 is the kinetic energy normalized to the electron rest energy. (a) Strong electric field, low injection energy, illustrating stochastic behavior. (b) Weak electric field, high injection energy, illustrating adiabatic behavior.

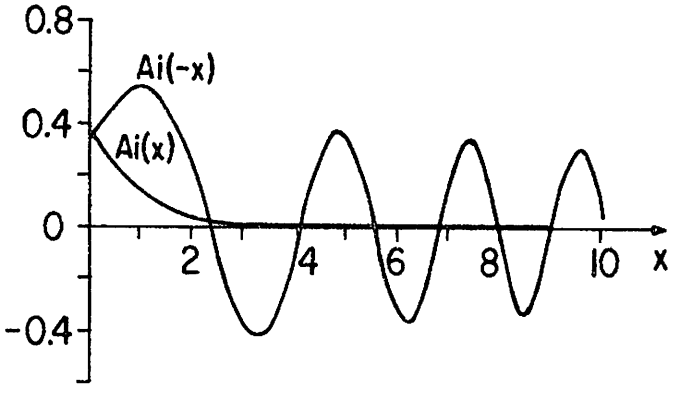

Fig. 2. The Airy function Ai(x) vs. x.

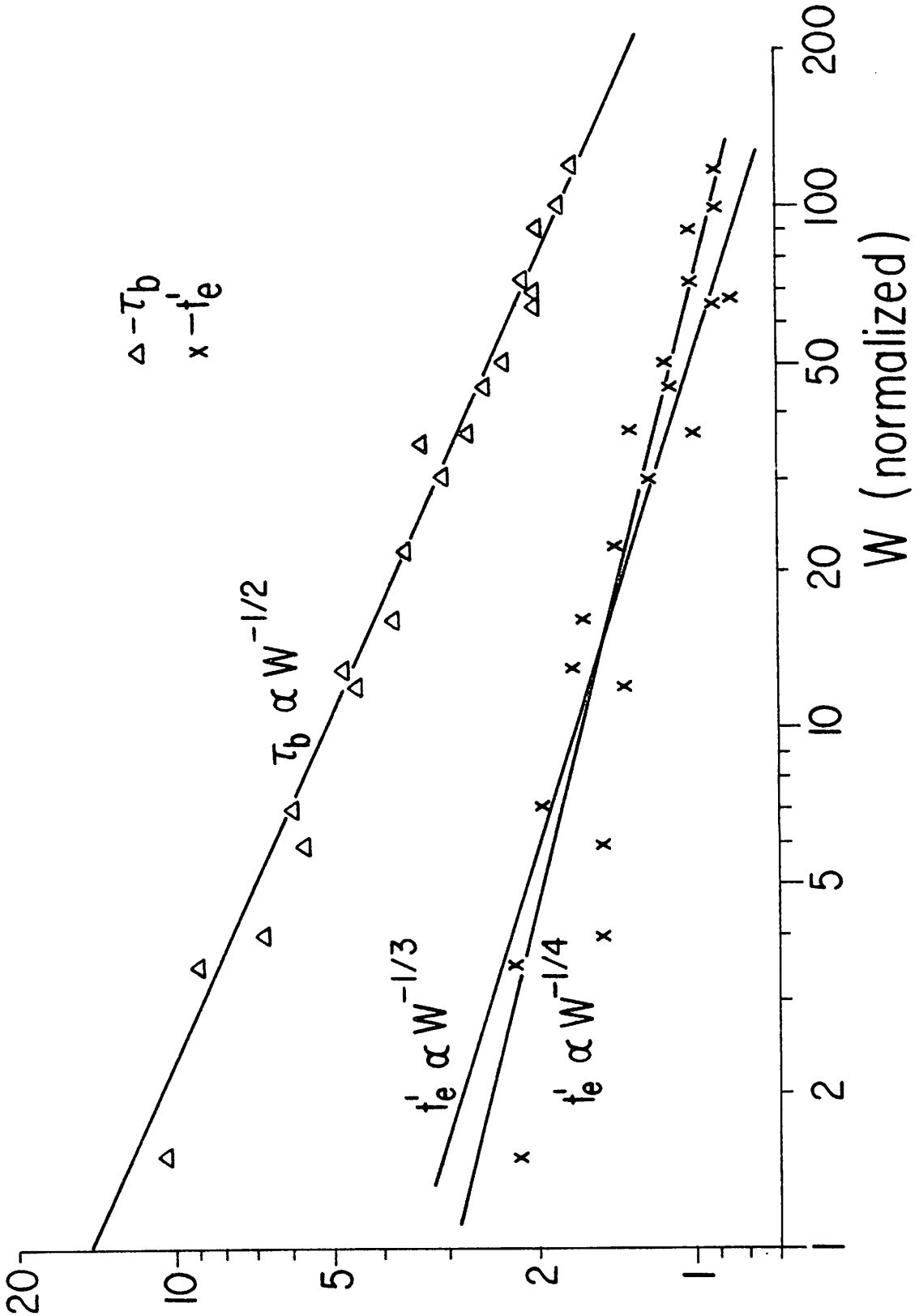

Fig. 3. The half-bounce time τ_b between successive crossings of the midplane and the time t'_e spent in the resonant zone, defined by π phase shift between rf and cyclotron phases, vs. particle energy W.

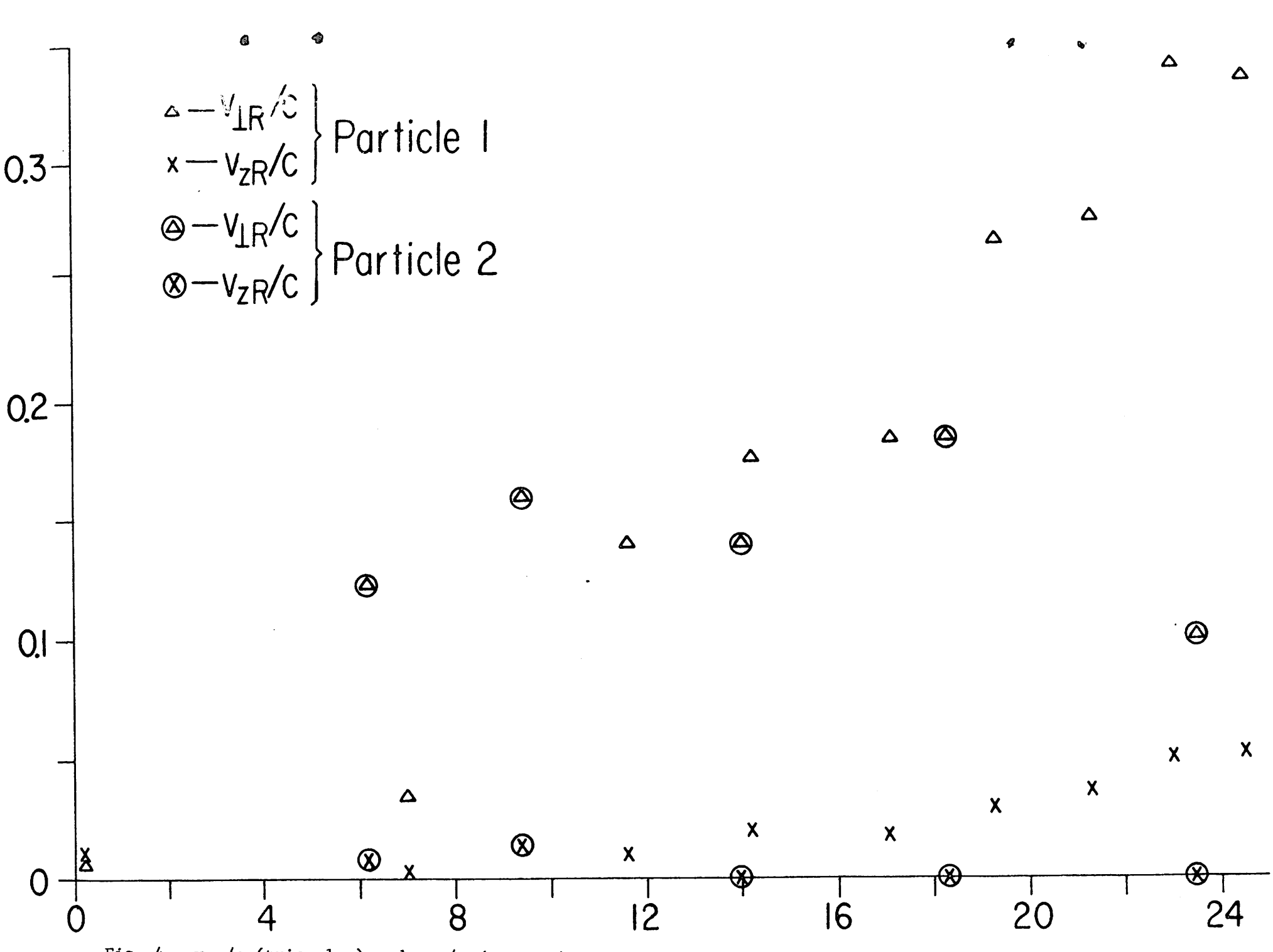

Fig. 4. $v_{\perp R}/c$ (triangles) and v_{zR}/c (crosses) vs. normalized time $\omega t/100$. ω is the rf driving frequency.

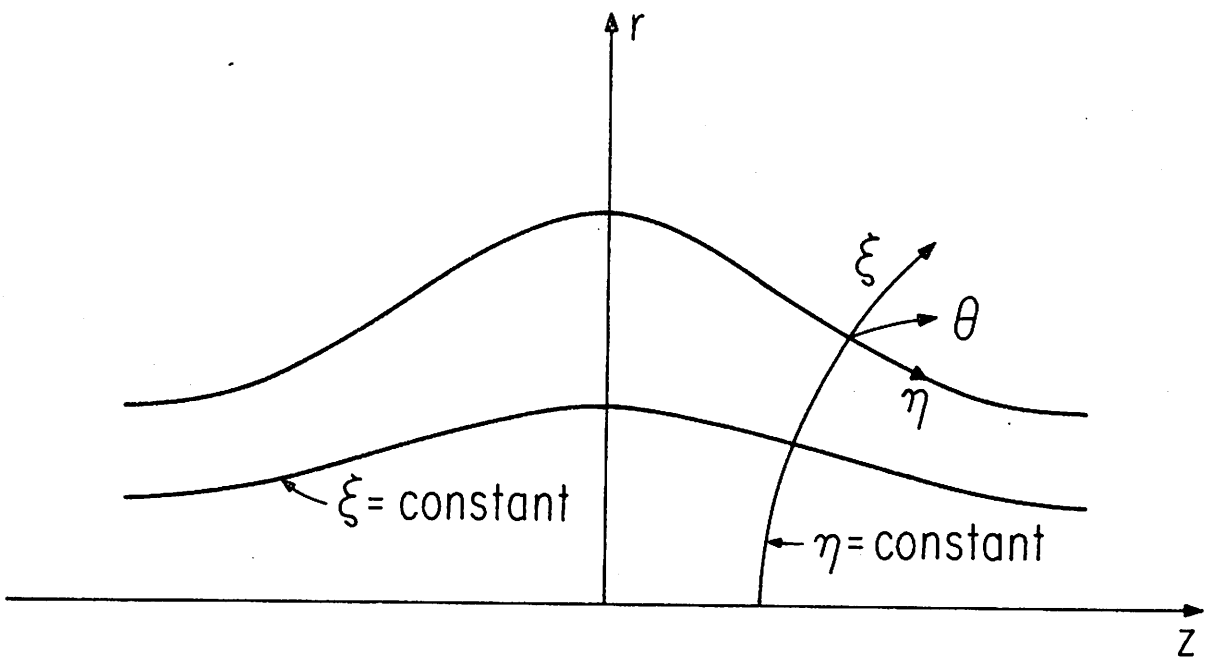

Fig. 5. Orthogonal coordinate system defined by the magnetic lines of force.

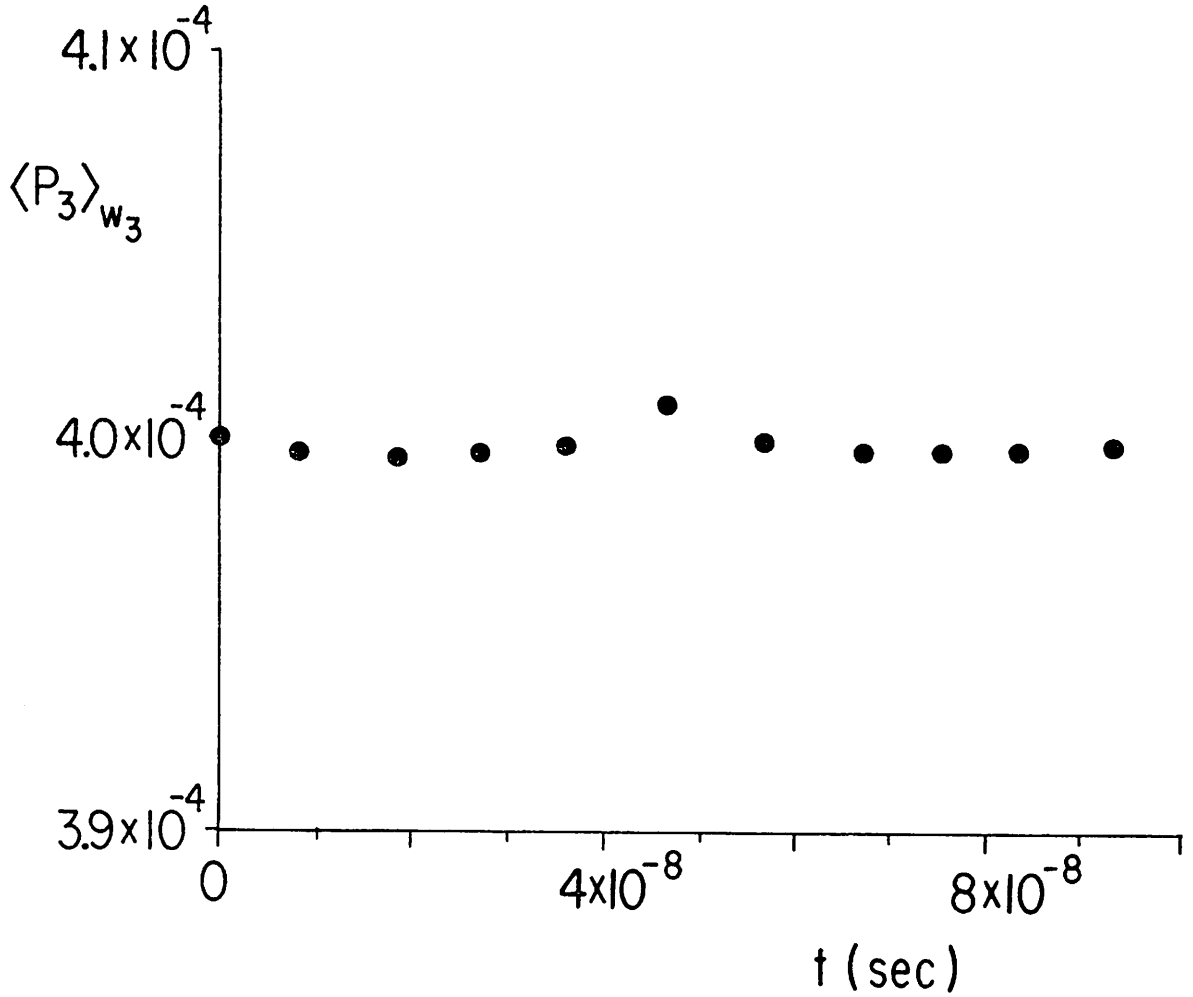

Fig. 6. Hamiltonian curves for electron cyclotron heating. (a) After averaging over both the cyclotron and bounce periods, from (39); (b) After averaging over the cyclotron period, but before averaging over the bounce period, from (36). (c) Phase plot of the exact equations of motion (1) and (2) for electron cyclotron heating with the perturbing rf field small ($\varepsilon = 10^{-5}$).

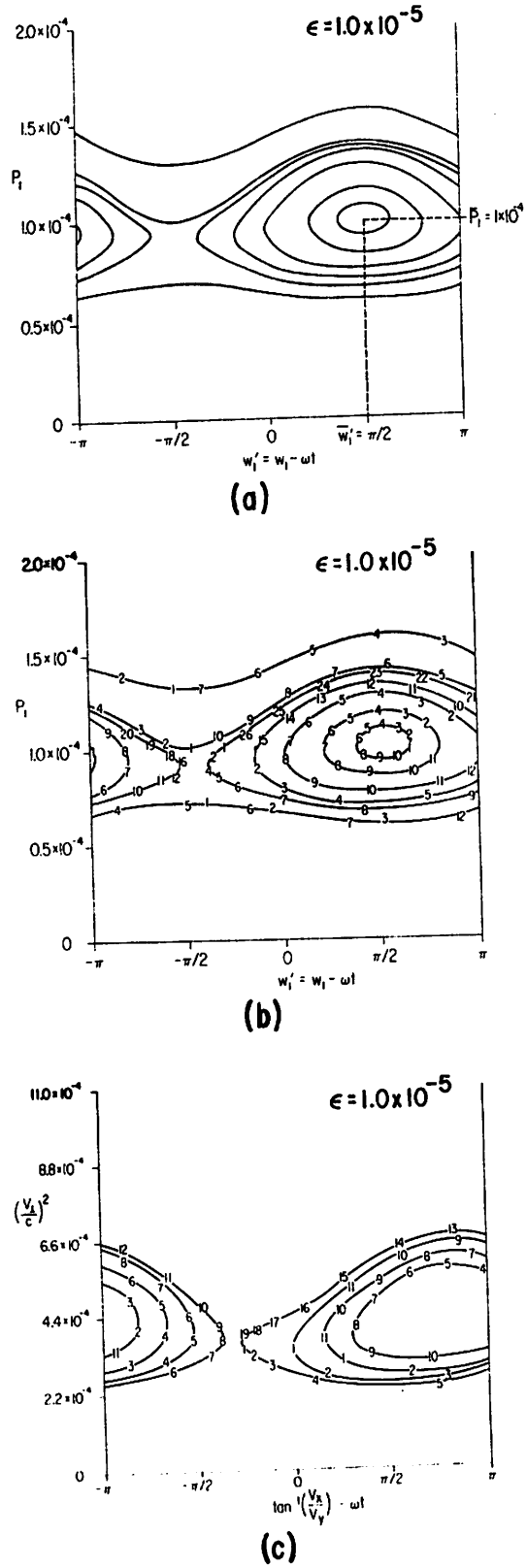

Fig. 7. Plot of adiabatic invariant of the bounce motion, P_3, as a function of time, for $\varepsilon = 10^{-5}$.

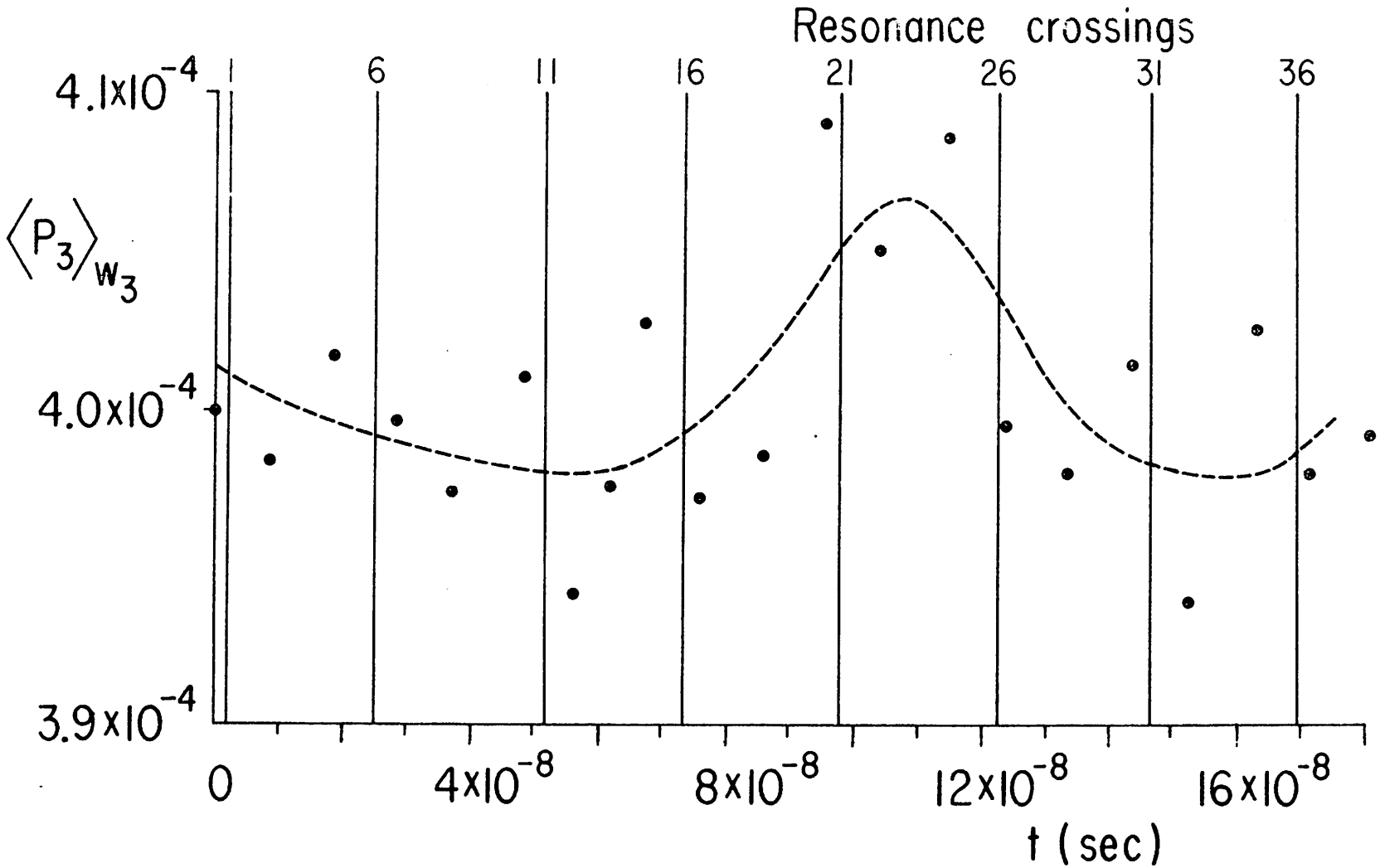

Fig. 8. Hamiltonian curves for electron cyclotron heating for which the perturbing rf field is large ($\varepsilon = 4.7 \times 10^{-5}$). (a) After averaging over both the cyclotron and bounce periods, from (39); (b) After averaging over the cyclotron period, but before averaging over the bounce period, from (36); (c) Phase plot of the exact equations of motion (1) and (2).

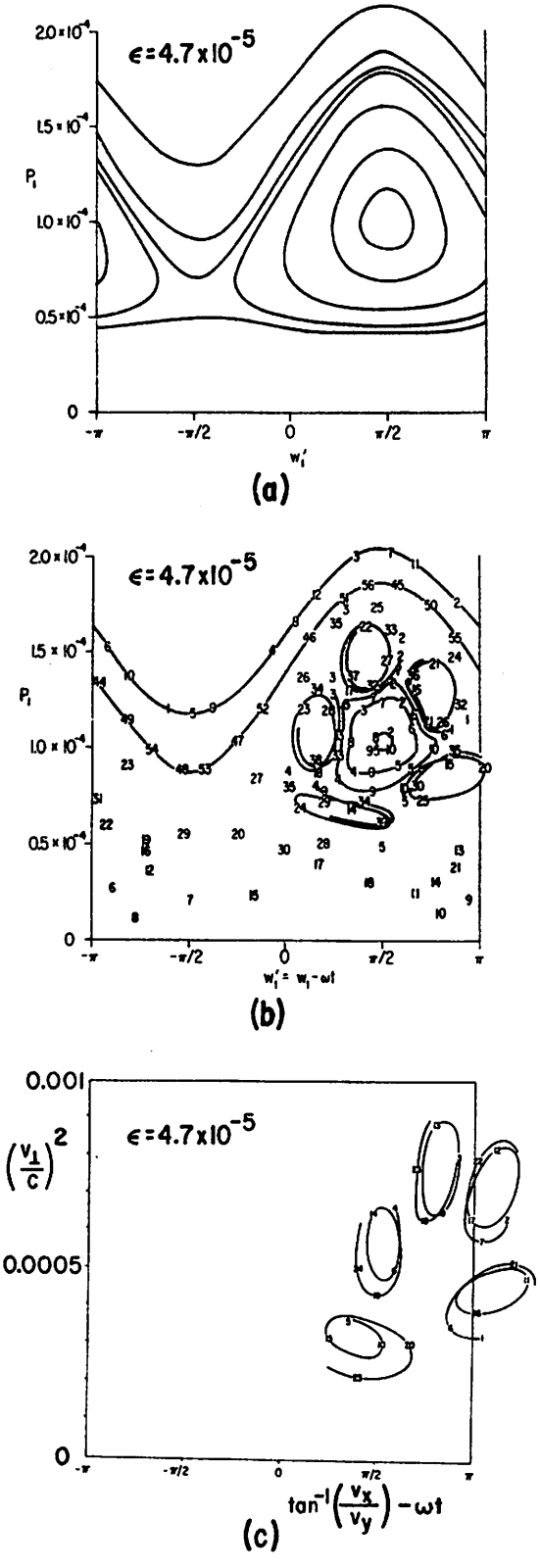

Fig. 9. Plot of adiabatic invariant of the bounce motion, P_3, as a function of time, for $\epsilon = 4.7 \times 10^{-5}$. The points are calculated over a complete bounce period or two resonance crossings.

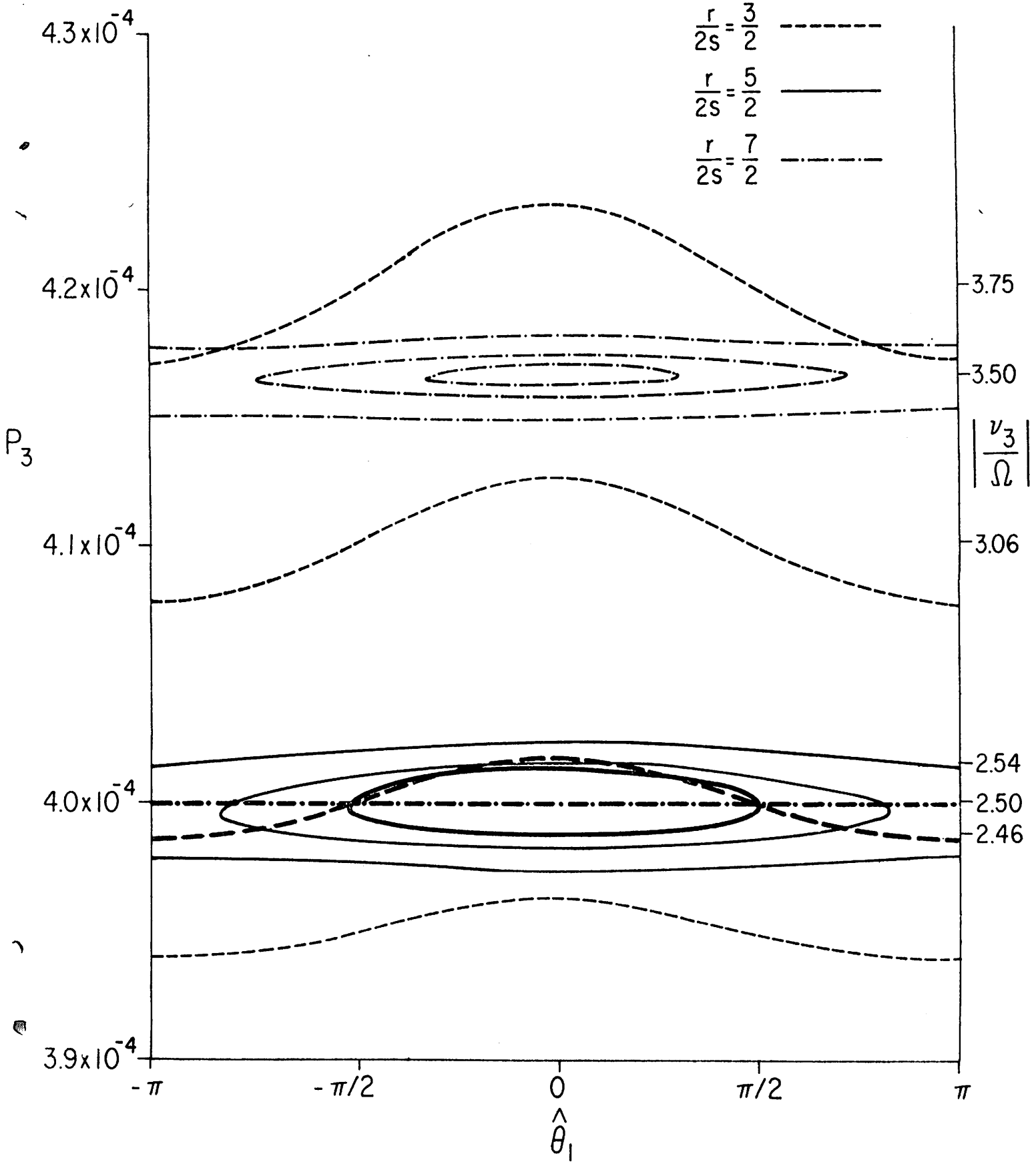

Fig. 10. Phase space of the oscillation of the longitudinal invariant due to resonance corresponding to the islands of Fig. 8b.

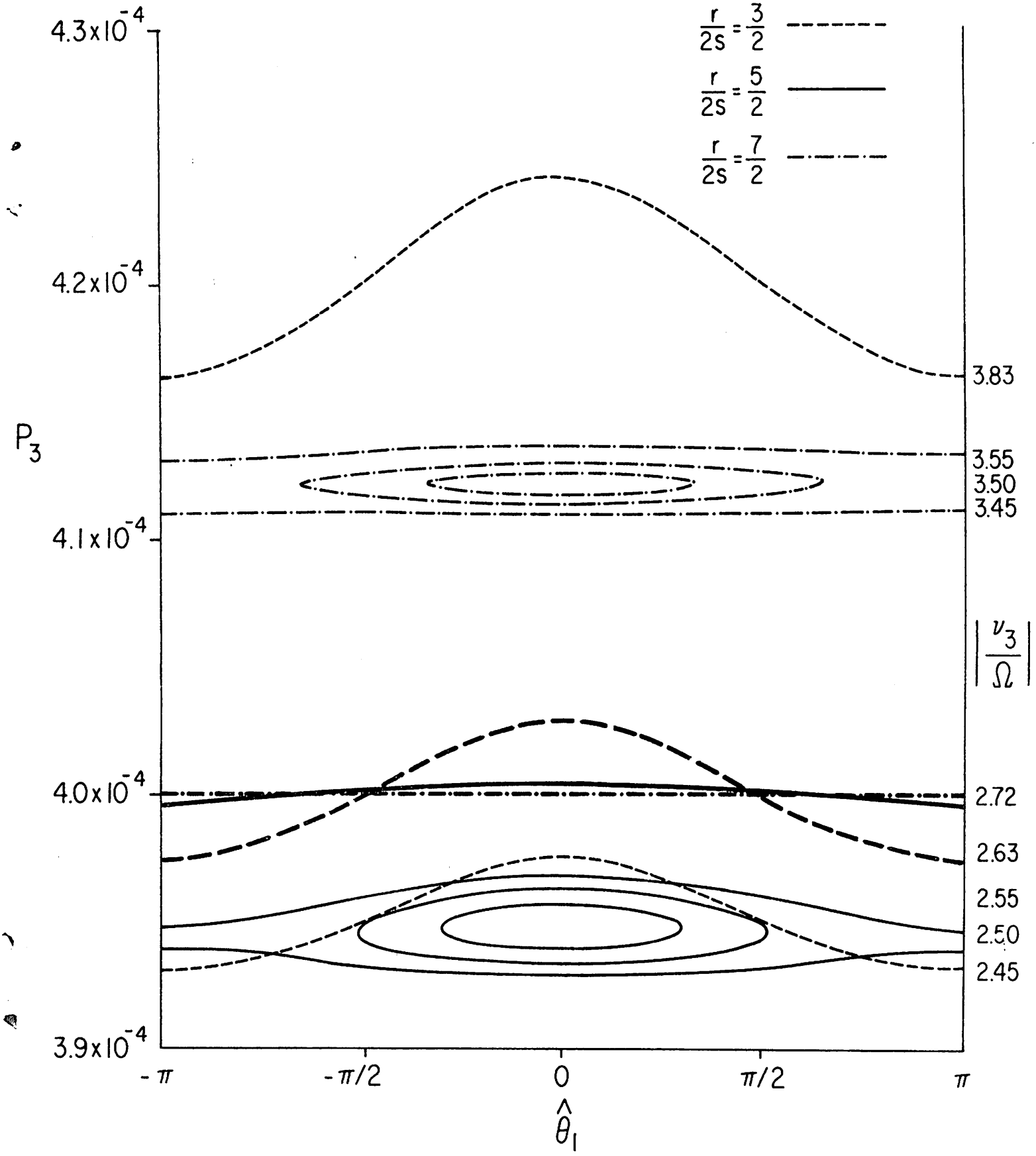

Fig. 11. Phase space of the longitudinal invariant corresponding to random motion in Fig. 8b.

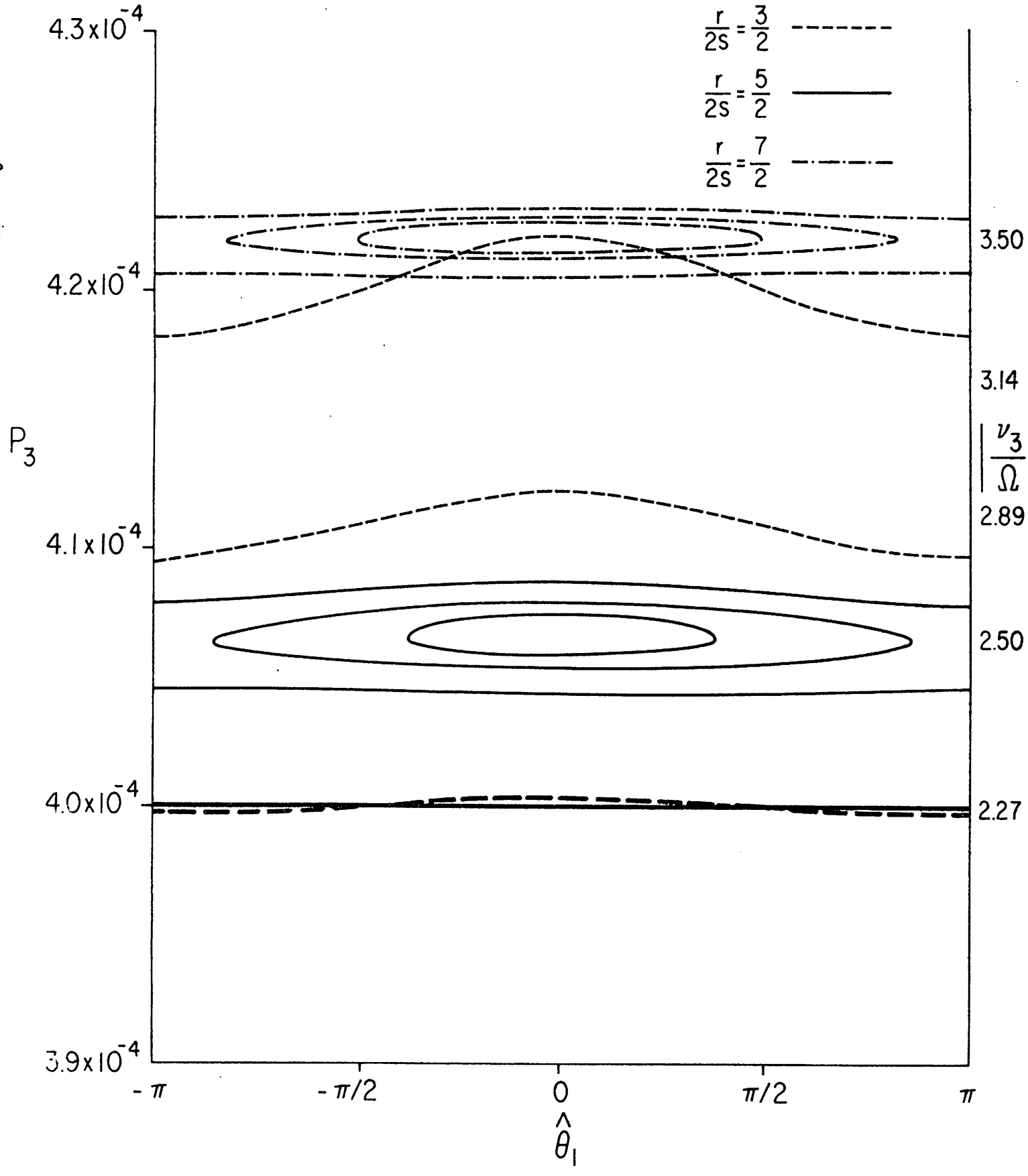

Fig. 12. Phase space of the longitudinal invariant corresponding to the well-behaved curves near the elliptic singularity of Fig. 8b.